



Elettra Sincrotrone Trieste

Basic concepts for LEEM, XPEEM and applications

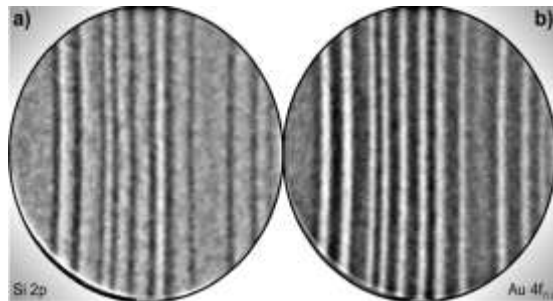
Andrea Locatelli

Andrea.locatelli@elettra.eu

Why do we need photoelectron microscopy?

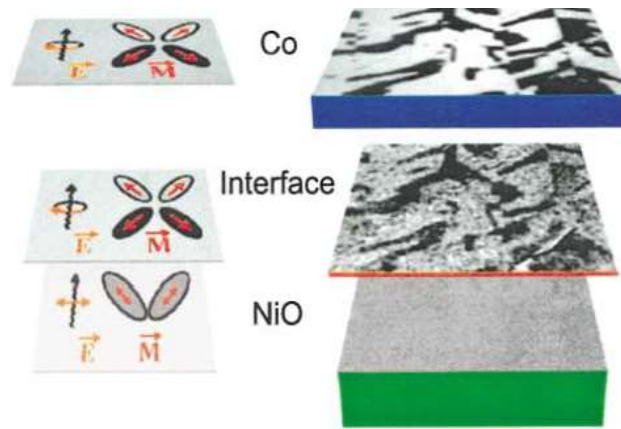
- To combine SPECTROSCOPY and MICROSCOPY to characterise the structural, chemical and magnetic properties of surfaces, interfaces and thin films
- Applications in diverse fields such as surface science, catalysis, material science, magnetism but also geology, soil sciences, biology and medicine.

Surface Science



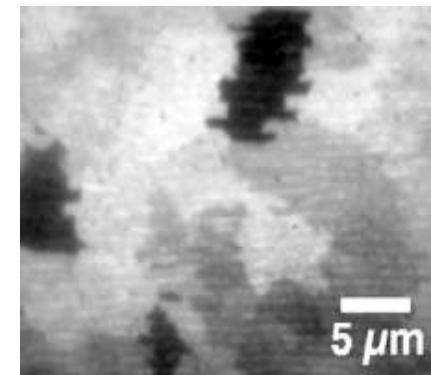
DOI: 10.1103/PhysRevLett.86.5088

Magnetism



DOI: 10.1103/PhysRevLett.87.247201

Biology



PRL 98, 268102 (2007)

Why does PEEM need synchrotron radiation?



Elettra Sincrotrone Trieste

- **High intensity** of SR makes measurements faster
- **Tuneability** – very broad and continuous spectral range from IR to hard X-Rays
- Narrow angular collimation
- Coherence!
- **High degree of polarization**
- **Pulsed time structure** of SR – This adds time resolution to photoelectron spectroscopy!
- Quantitative control on SR parameters allows spectroscopy:
 - Absorption Spectroscopy (XAS and variants)
 - Photoemission Spectroscopies (XPS, UPS, ARPES, ARUPS)

$$J = f(h\nu, \varepsilon, \Theta, \Phi; E_{kin}^e, \sigma, \theta_e, \varphi_e)$$

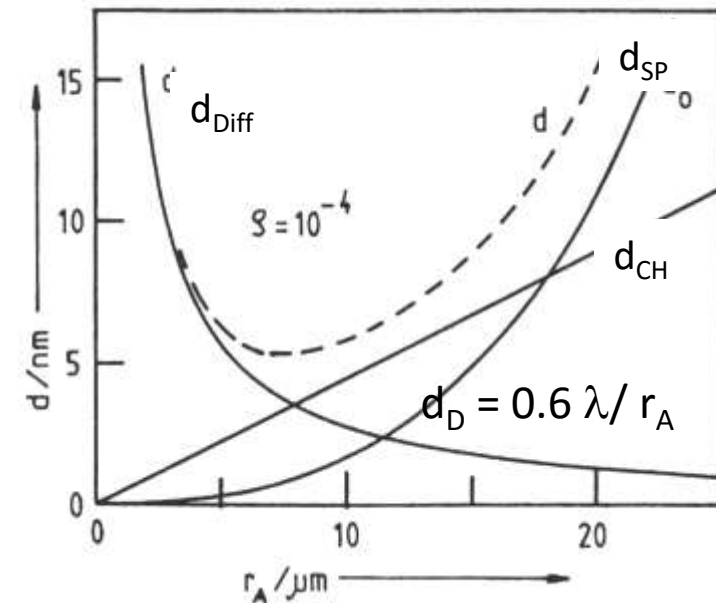
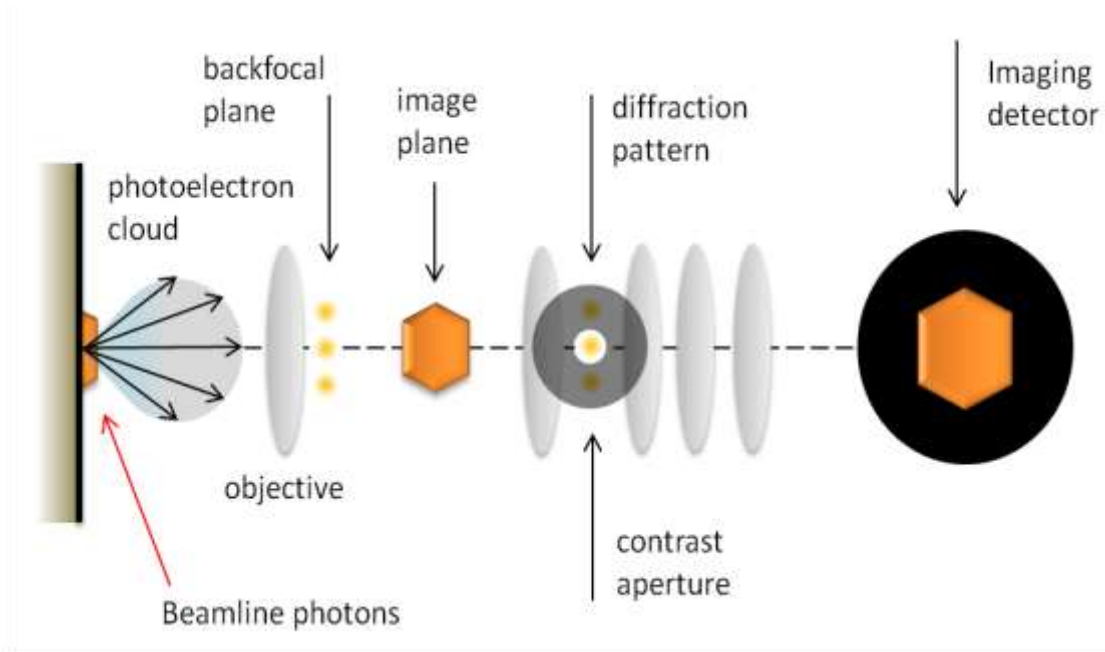
Outline

- Synchrotron radiation and x-ray spectro-microscopy: basics
- Cathode lens microscopy: methods
- Applications
 - Chemical imaging of micro-structured materials
 - Graphene research.
 - Magnetism
 - Time-resolved XPEEM



Cathode lens microscopy methods

PEEM, LEEM, SPELEEM, AC-PEEM/LEEM



$$d = \sqrt{d_{SP}^2 + d_{CH}^2 + d_D^2}$$

PEEM is a full-field technique. The microscope images a restricted portion of the specimen area illuminated by x-ray beam. Photoemitted electrons are collected at the same time by the optics setup, which produces a magnified image of the surface. The key element of the microscope is the objective lens, also known as cathode or immersion lens, of which the sample is part

The different types of PEEM measurements



Elettra Sincrotrone Trieste

PEEM

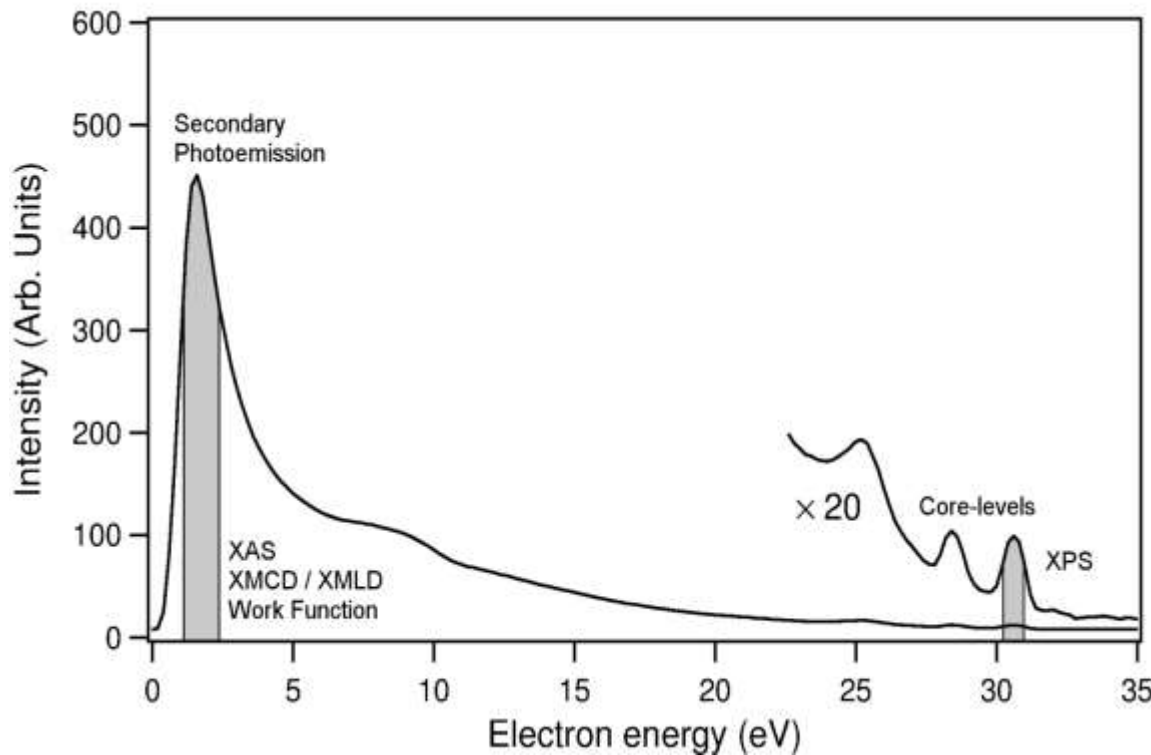
- threshold microscopy
- Laterally resolved XPS, micro-spectroscopy
- Laterally resolved UPS, microprobe ARUPS /ARPES
- Auger Spectroscopy
- XAS-PEEM (XMC/LD-PEEM)

Probe

- Hg lamp
- X-ray
- X-rays, He lamp
- X-ray, or electrons
- X rays

Measurement

- photoelectrons
- core levels or VB ph.el.
- VB photoelectrons
- secondary electrons
- secondary electrons

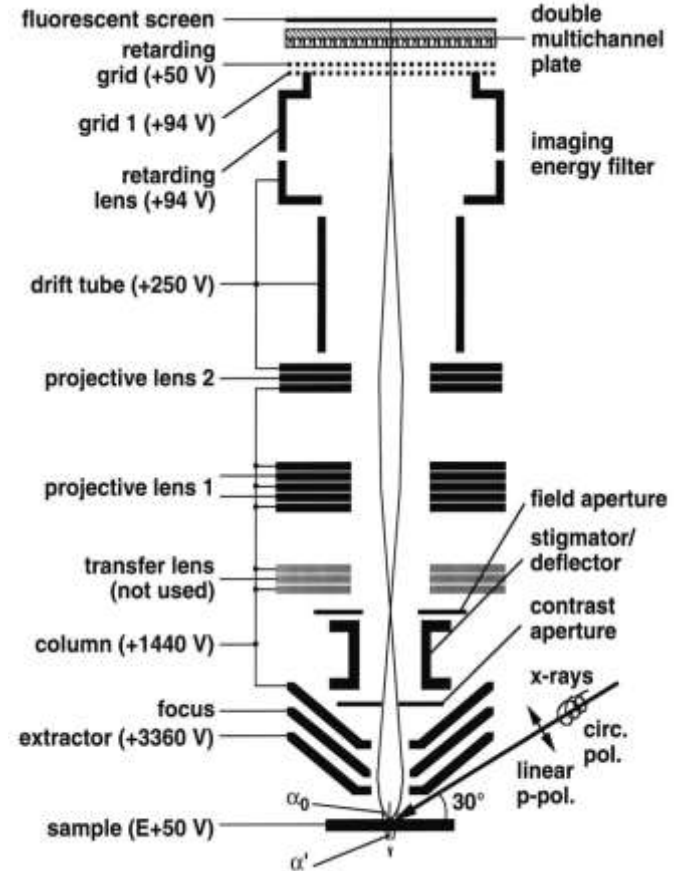
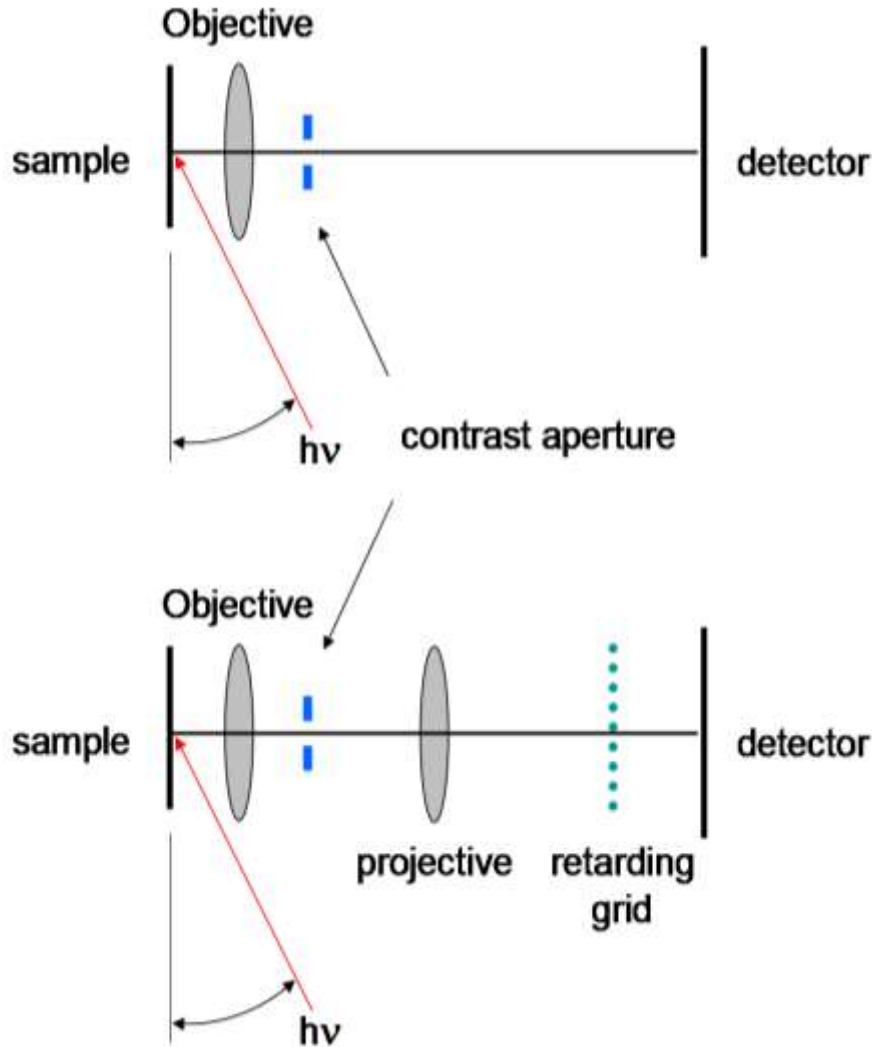


Require energy filter

Simple PEEM instruments



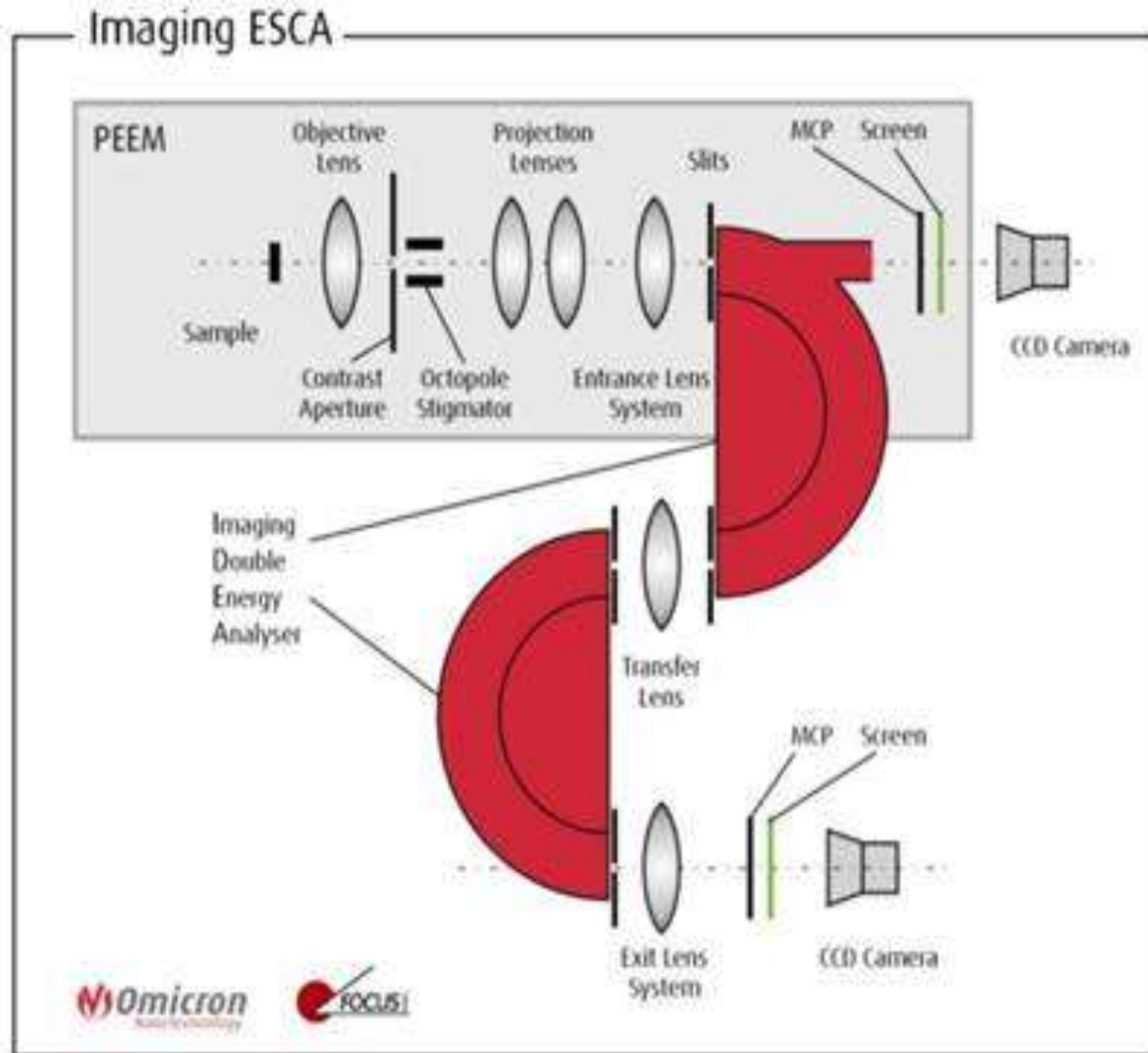
Elettra Sincrotrone Trieste

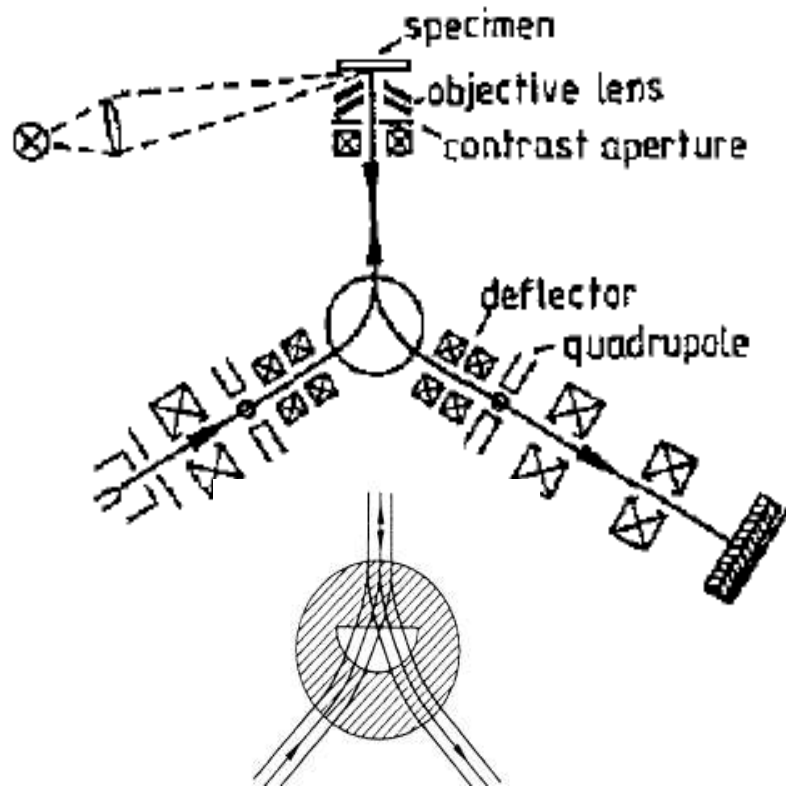


PEEM instruments with energy filter: NanoESCA

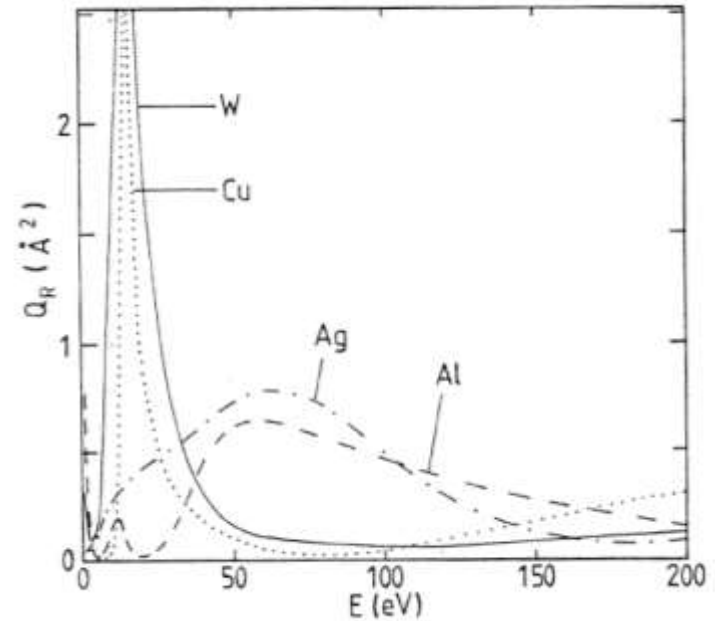


Elettra Sincrotrone Trieste





Backscattering cross section



E. Bauer, Rep. Prog. Phys. 57 (1994) 895-938.

- LEEM probes surfaces with low energy electrons, using the elastically backscattered beam for imaging.
- Direct imaging and diffraction imaging modes

- High structure sensitivity
- High surface sensitivity
- Video rate: reconstructions, growth, step dynamics, self-organization

Imaging dynamic processes in LEEM

$540 < T < 750 \text{ C}$

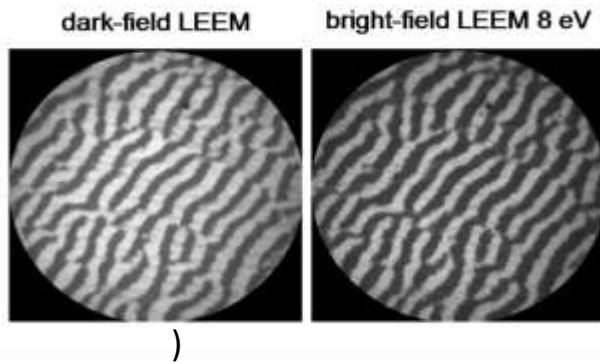


Ni growth on W(110): step flow and completion of ps ML

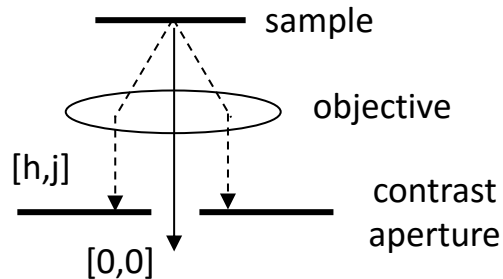
Ni growth on W(110): formation of a striped phase above 1 ps ML Ni

Different contrast mechanisms are available for structure characterization

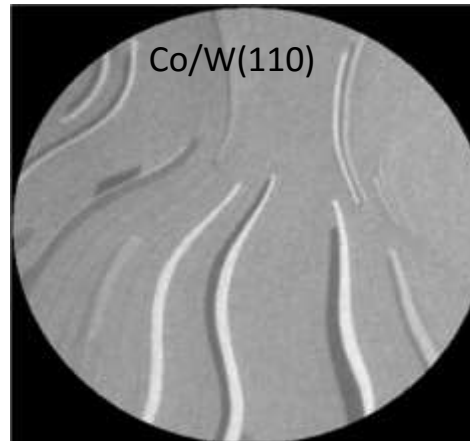
SURFACE STRUCTURE



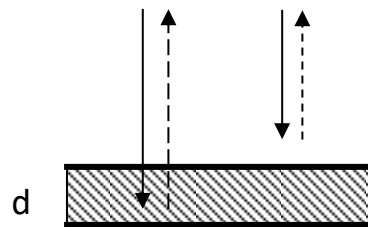
diffraction
contrast



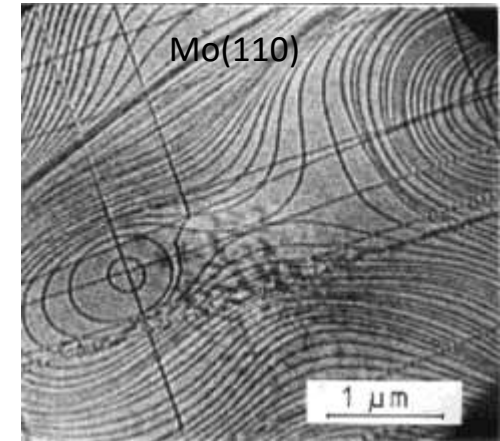
FILM THICKNESS



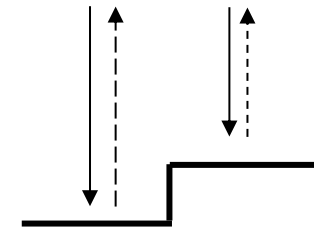
quantum size
contrast



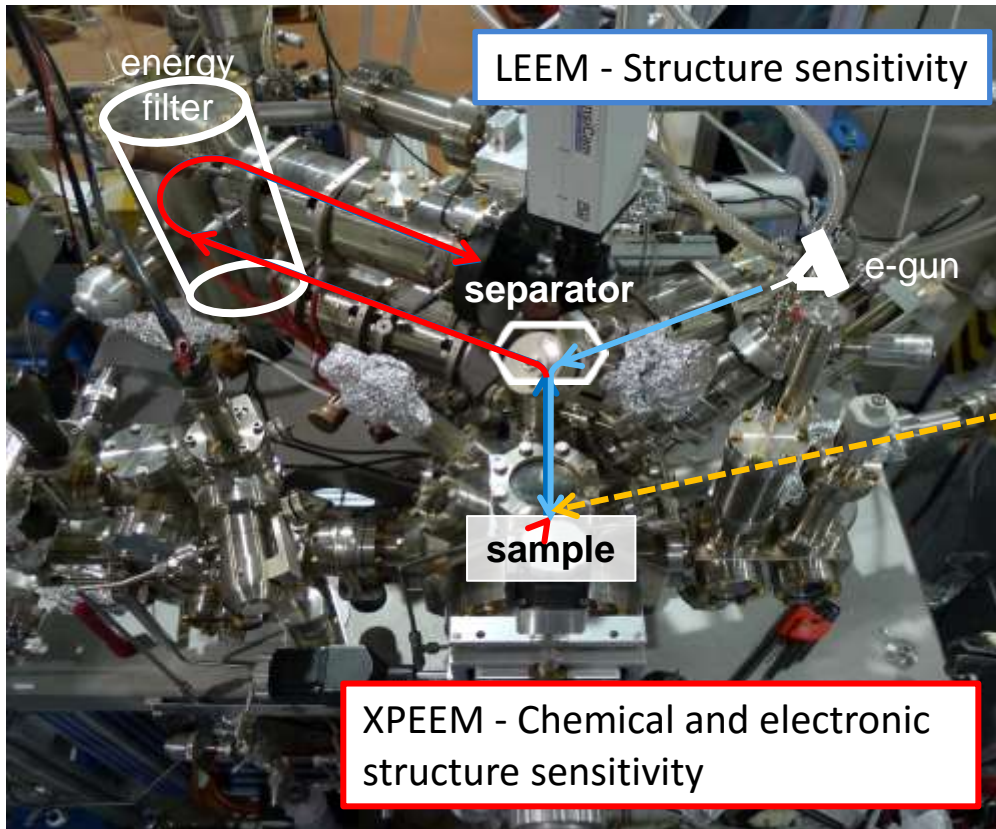
STEP MORPHOLOGY



geometric
phase contrast

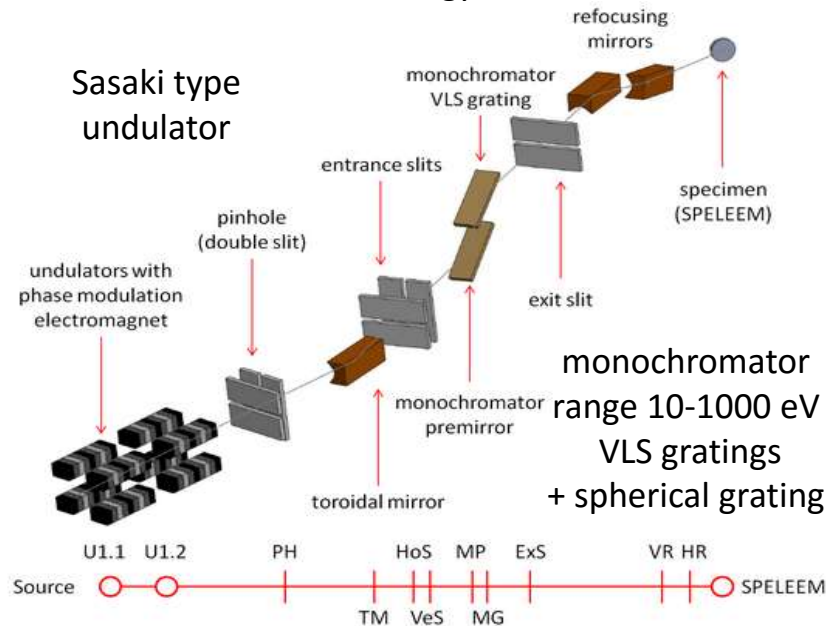


SPELEEM = LEEM + PEEM



The Nanospectroscopy beamline@Elettra

Flux on the sample: 10^{13} ph/sec (microspot)
intermediate energy resolution.



Applications:

characterization of materials at microscopic level, magnetic imaging of micro-structures
Imaging of dynamical processes

A. Locatelli, L. Aballe, T.O. Menteş, M. Kiskinova, E. Bauer, Surf. Interface Anal. 38, 1554-1557 (2006)

T. O. Menteş, G. Zamborlini, A. Sala, A. Locatelli; Beilstein J. Nanotechnol. 5, 1873-1886 (2014)

SPELEEM many methods analysis

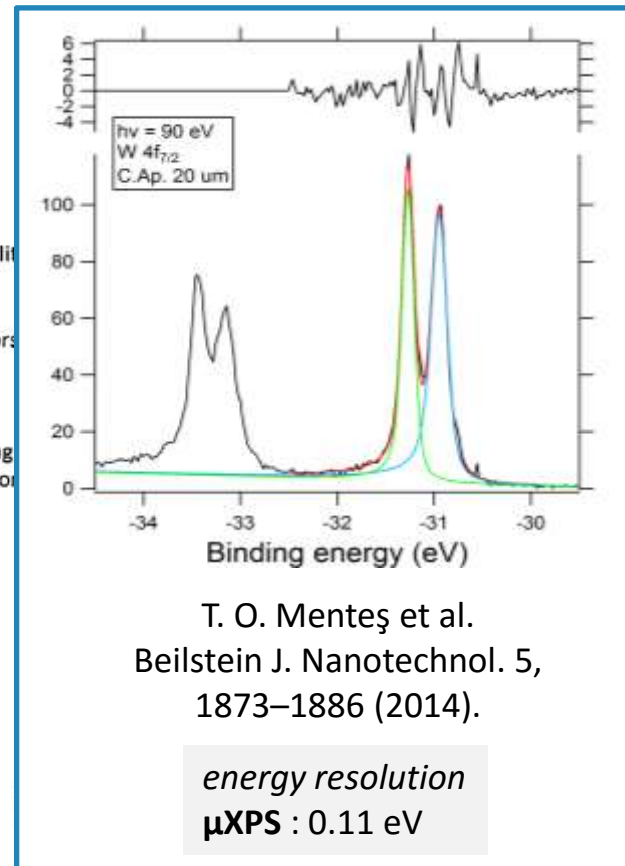
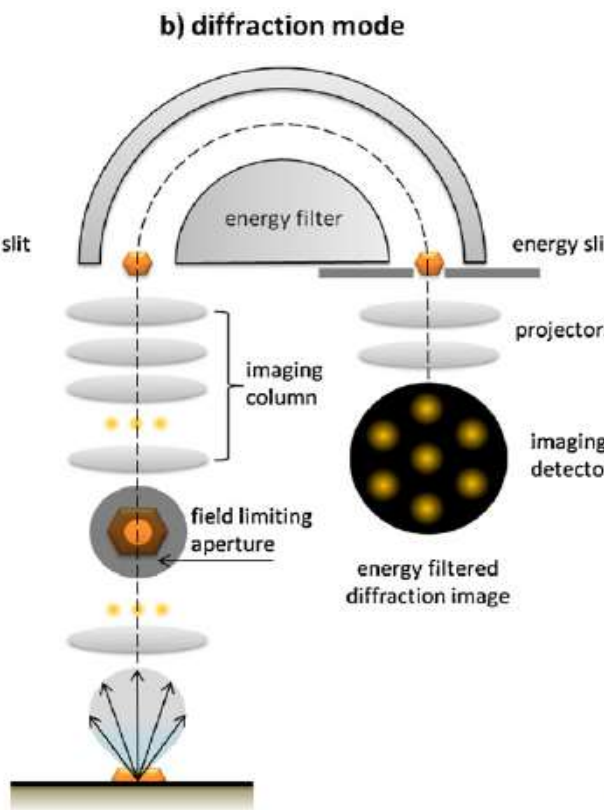
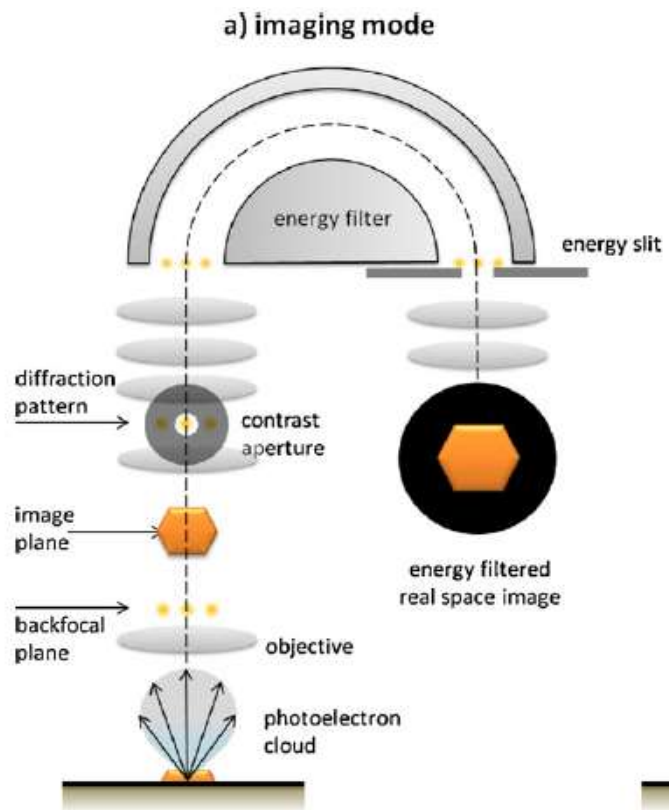


Elettra Sincrotrone Trieste

Spectroscopic imaging
XAS-PEEM / XPEEM / LEEM

microprobe-diffraction
ARPES / LEED

microprobe-spectroscopy
XPS



T. O. Menteş et al.
Beilstein J. Nanotechnol. 5,
1873–1886 (2014).

energy resolution
 μ XPS : 0.11 eV

spatial resolution
LEEM : 10 nm
XPEEM : 25 nm

energy resolution
XPEEM : 0.3 eV

Limited: to 2 microns in dia.
angular resolution
transfer width: 0.01 \AA^{-1}

Performance: lateral resolution in imaging: **10nm** (LEEM)
30 nm (XPEEM)
energy resolution: **0.3 eV** (0.1 eV muXPS)

Key feature: multi-method instrument to the study of surfaces and interfaces offering *imaging* and *diffraction* techniques.

Probe: *low energy e-* (0-500 eV) \longleftrightarrow structure sensitivity
soft X-rays (50-1000 eV) \longleftrightarrow chemical state, magnetic state, electronic struct.

Applications: *characterization* of materials at microscopic level
magnetic imaging of microstructures
dynamical processes

Correction of spherical and chromatic aberrations



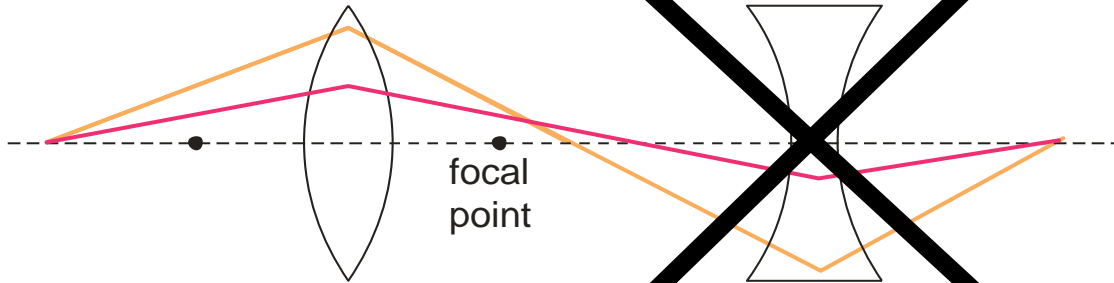
Elettra Sincrotrone Trieste

Electron optics

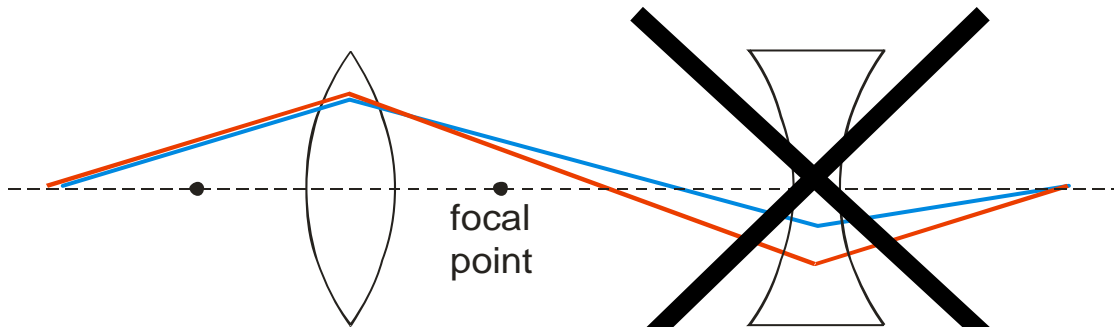
Round **convex** lenses

Round **concave** lenses

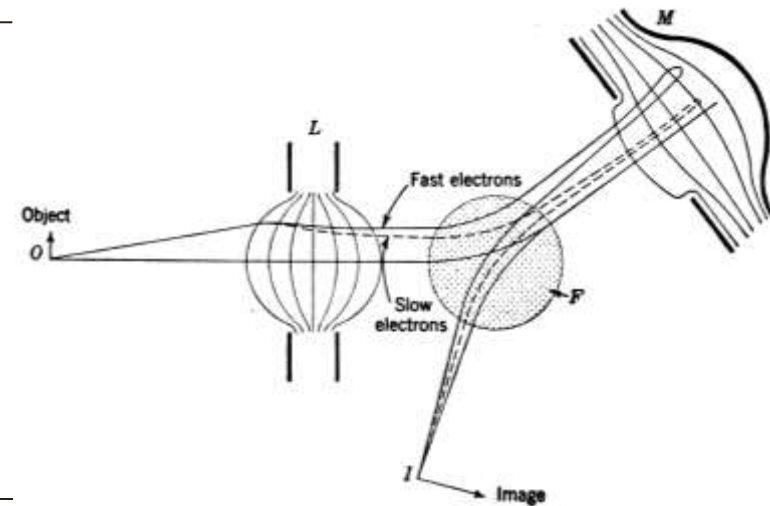
Electron Mirror



Spherical aberration



Chromatic aberration



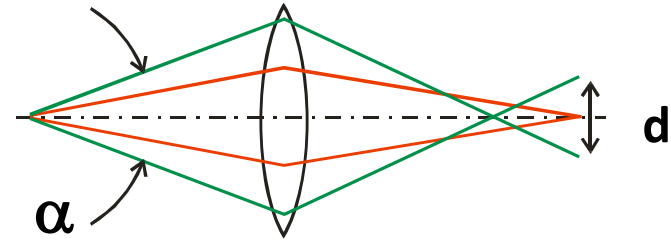
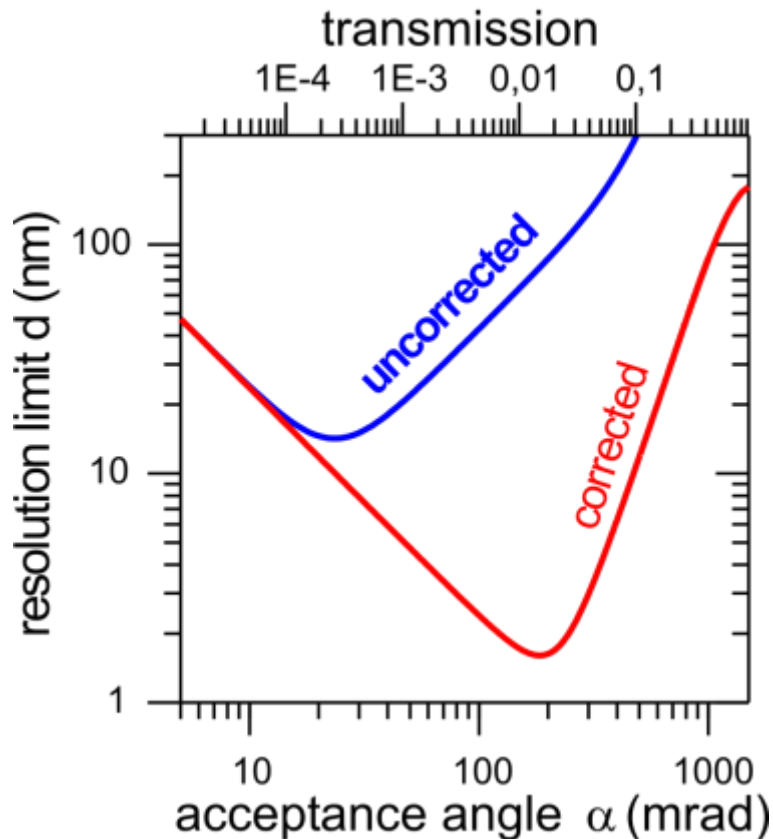
V.K. Zworykin et al, Electron Optics and the Electron Microscope, John Wiley, New York 1945

The SMART AC microscope: calculation



Elettra Sincrotrone Trieste

Simultaneous improvement in Transmission and Resolution!!!



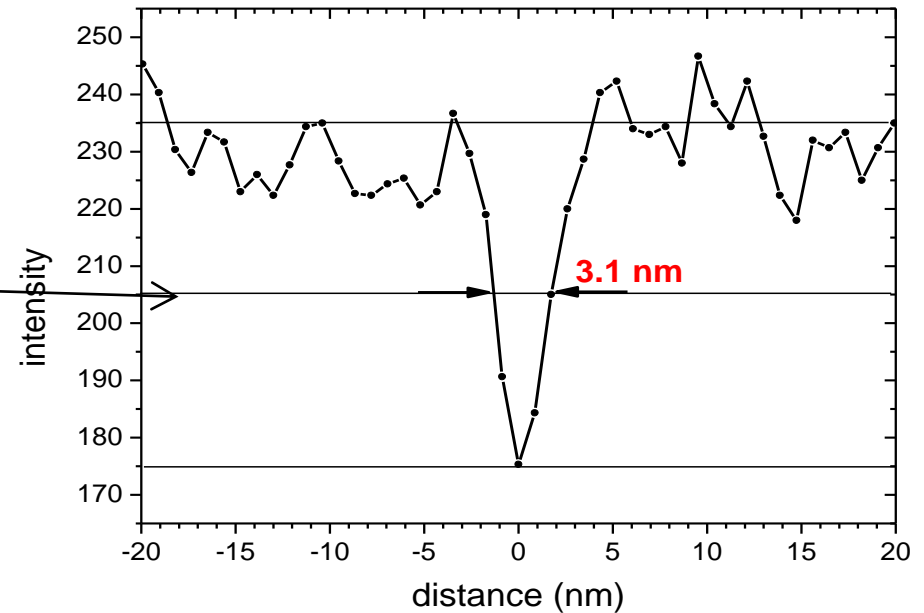
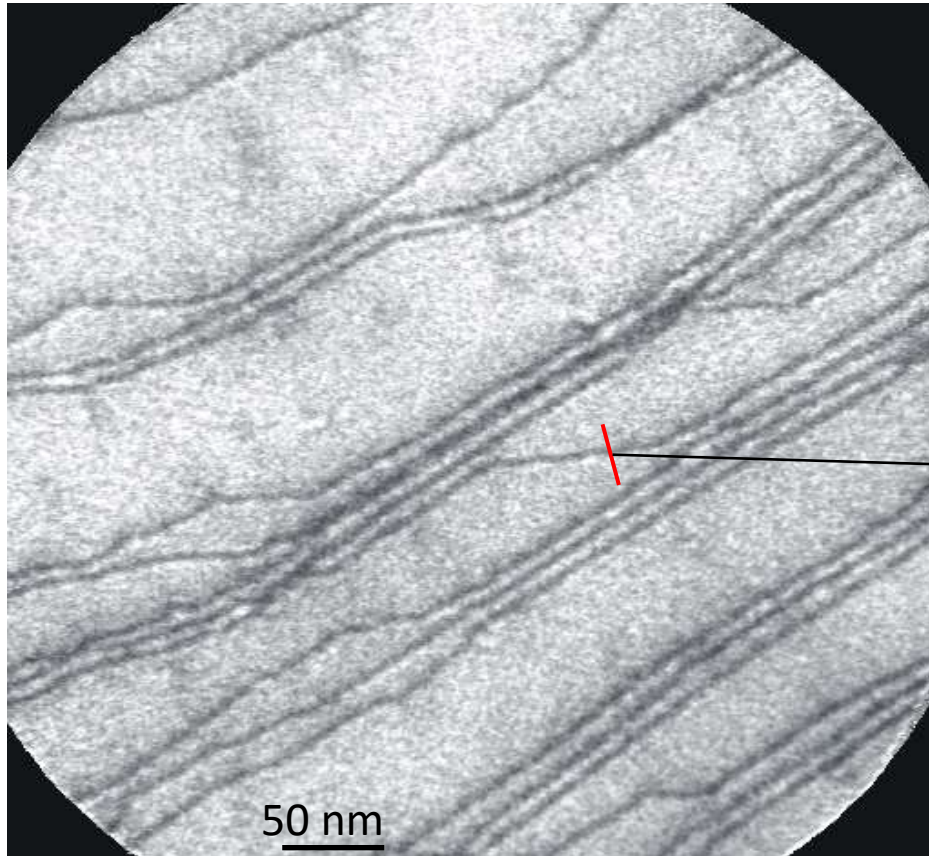
Resolution limit	without correction	with correction
Spherical	$\alpha^3 + \dots$	α^5
Chromatic	$\Delta E \alpha + \dots$	$\Delta E \alpha^2 + \Delta E^2 \alpha$
Diffraction	$1/\alpha$	$1/\alpha$

D. Preikszas, H. Rose, J. Electr. Micr. 1 (1997) 1

Th. Schmidt, D. Preikszas, H. Rose et al., Surf.Rev.Lett 9 (2002) 223

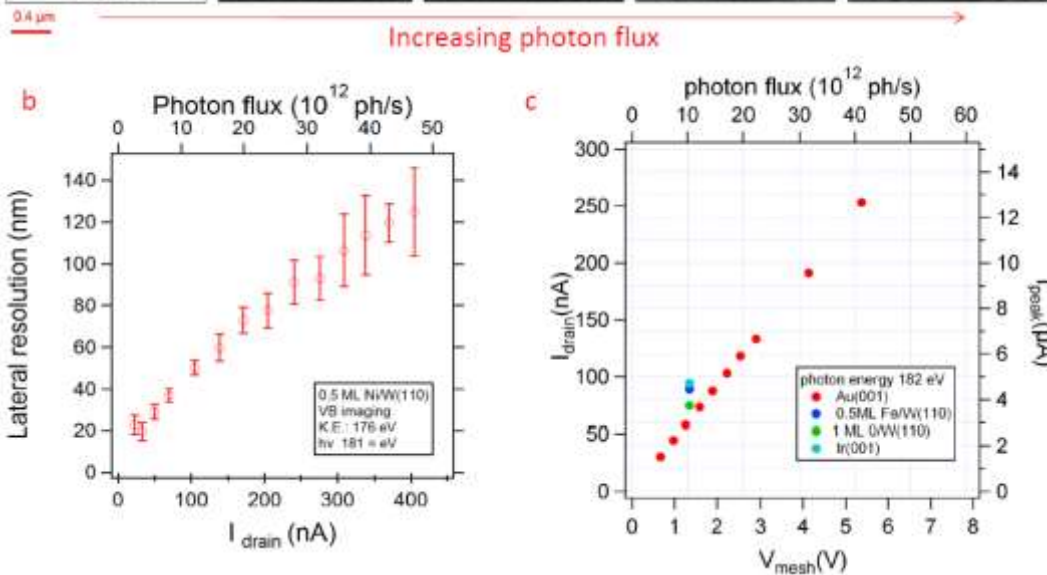
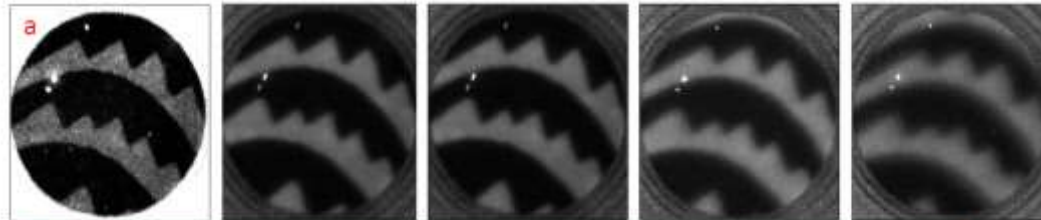
First results of the SMART microscope @BESSY

Atomic steps on Au(111),
LEEM 16 eV, FoV = 444 nm x 444 nm
(18.09.06)



Courtesy of Th. Schmidt et al.; 5th Int. Conf. LEEM/PEEM, Himeji, 15.-19. Oct. 2006

Ni/W(100) $h\nu = 181$ eV



photocurrent estimate for SPELEEM@Elettra; Au/W(110)

- 440 bunches
rev. frequency: 1.157 MHz
bunch length: 42 ps (2GeV)
- $1 \cdot 10^{13}$ ph./s on sample =
= 20000 ph./bunch
- Total photoionization yield:
about 2% photons result in a photoemission event
- $I_{\text{peak}} \approx 400 \text{ e}^- / 42 \text{ ps}$
 $\approx 1.5 \mu\text{A vs } 20 \text{ nA (LEEM)}$
 $13 \text{ pA}/\mu\text{m}^2 \text{ versus } 20 \text{ nA}/\mu\text{m}^2$

1. Image blur can be observed with SR but only under very high photon fluxes. Must Keep into account in beamline design. No space charge in LEEM
2. Both the lateral and energy resolution are strongly degraded by Boersch and Loeffler effects occurring in the first part of optical path.



Chemical imaging applications

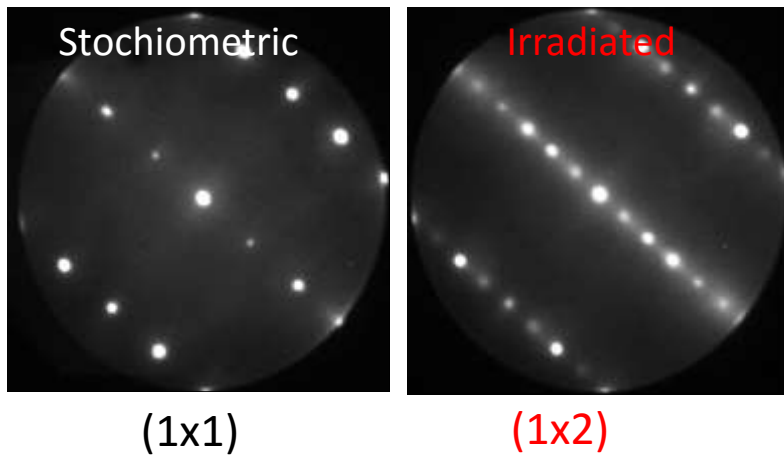
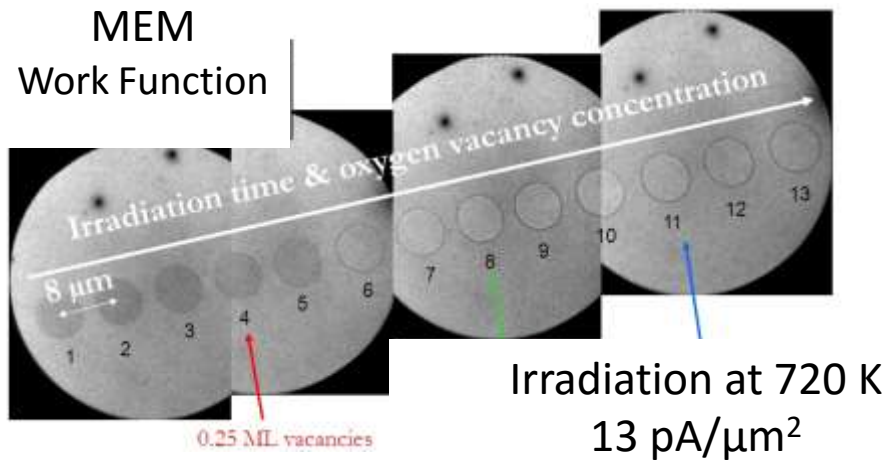
PEEM, LEEM, SPELEEM, AC-PEEM/LEEM

Au/TiO₂(110): controlling growth by vacancies

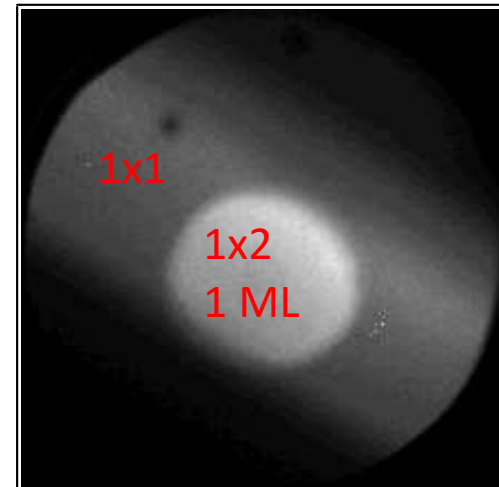


Elettra Sincrotrone Trieste

Creation of ordered oxygen vacancies

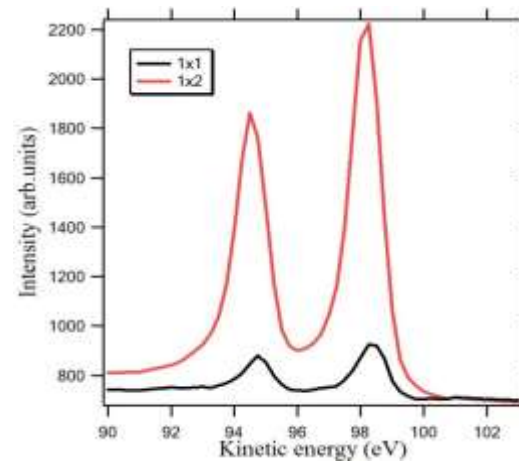


Au growth on TiO₂(110)



XPEEM
@ Au 4f

μ -LE
struc



μ -XPS

Surface Oxygen on Ag : *e*-beam "Lithography"

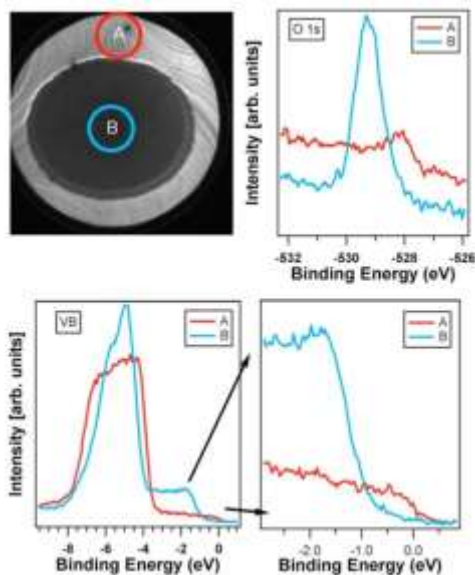


Elettra Sincrotrone Trieste

Full oxidation of Ag using NO₂ does not occur:



Instead: *e*-beam (60 eV) stimulated desorption of NO_{ad} works at RT!

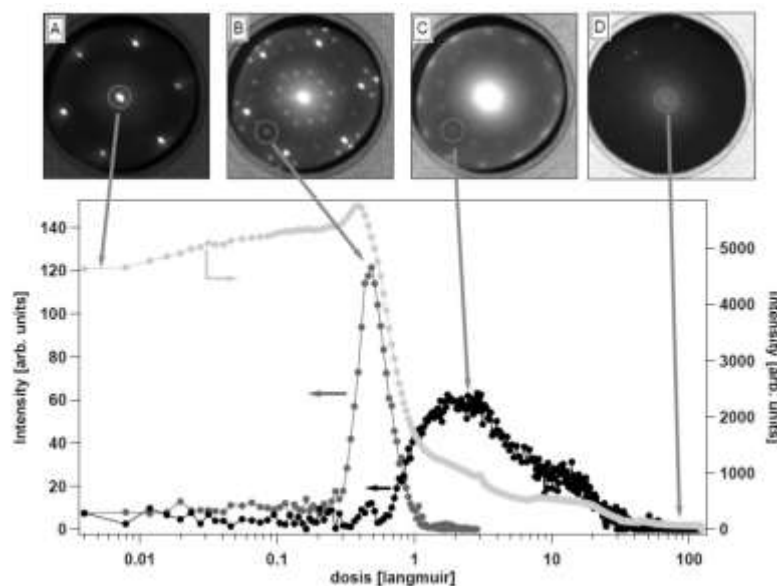


A: metallic Ag
B: Ag₂O

Low T: NO_{ad} stays, prevents oxidation.

High T: NO_{ad} desorbs, but Ag₂O unstable.

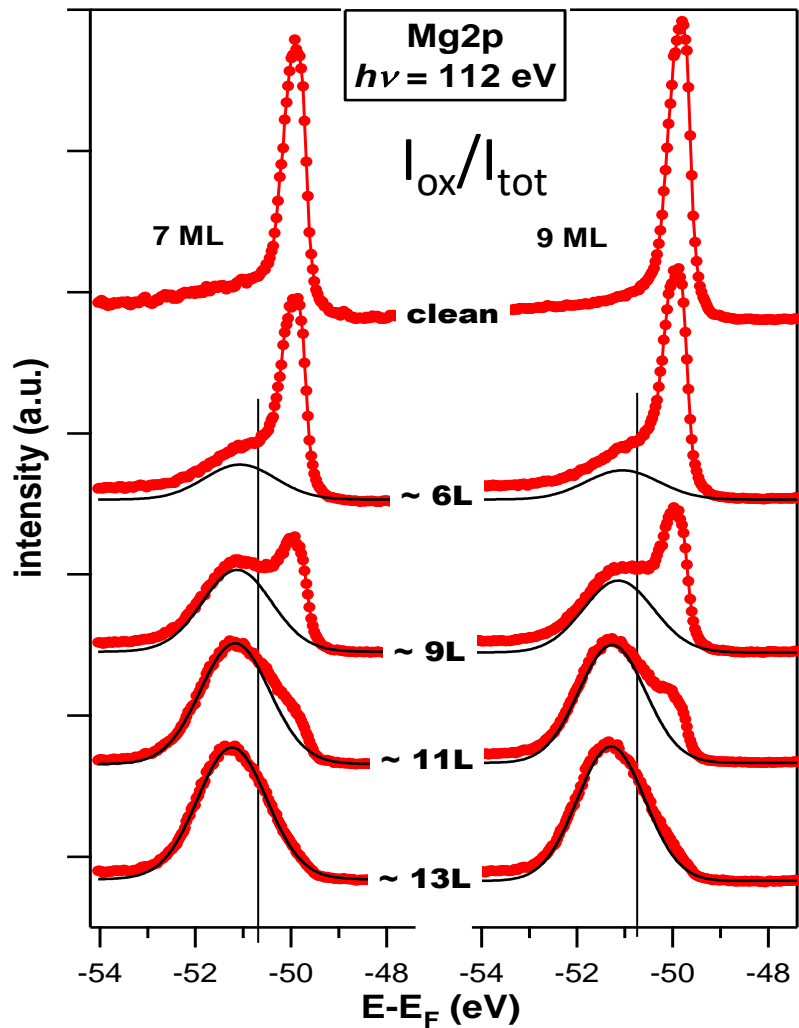
LEED reveals path towards Ag₂O under *e*-beam



S. Günther *et al.*, *App. Phys. Lett.* 93, 233117 (2008).

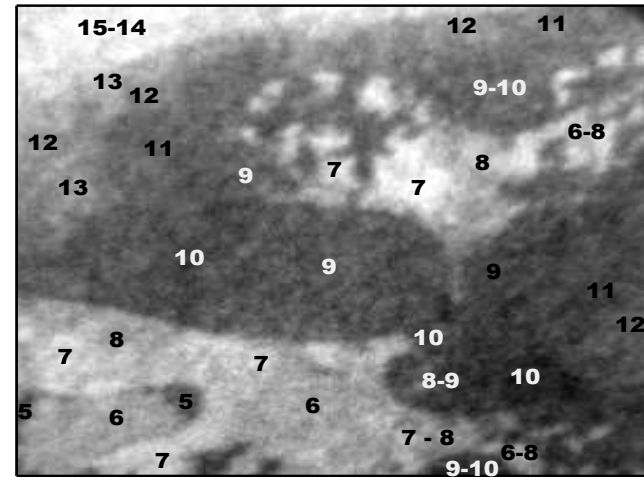
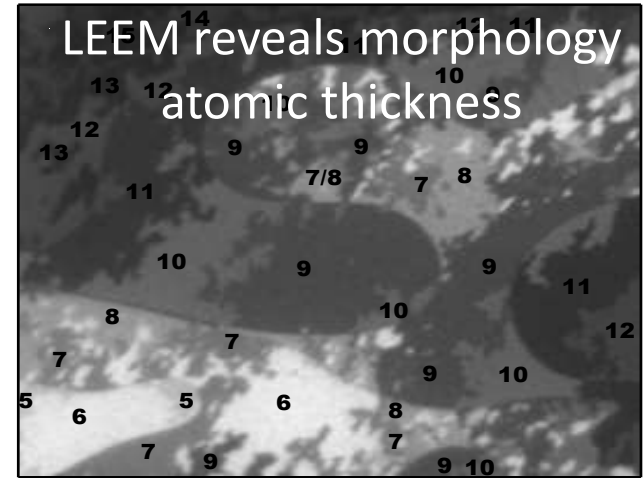
S. Günther *et al.*, *Chem. Phys. Chem.* 2010.

Thickness dependent reactivity in Mg

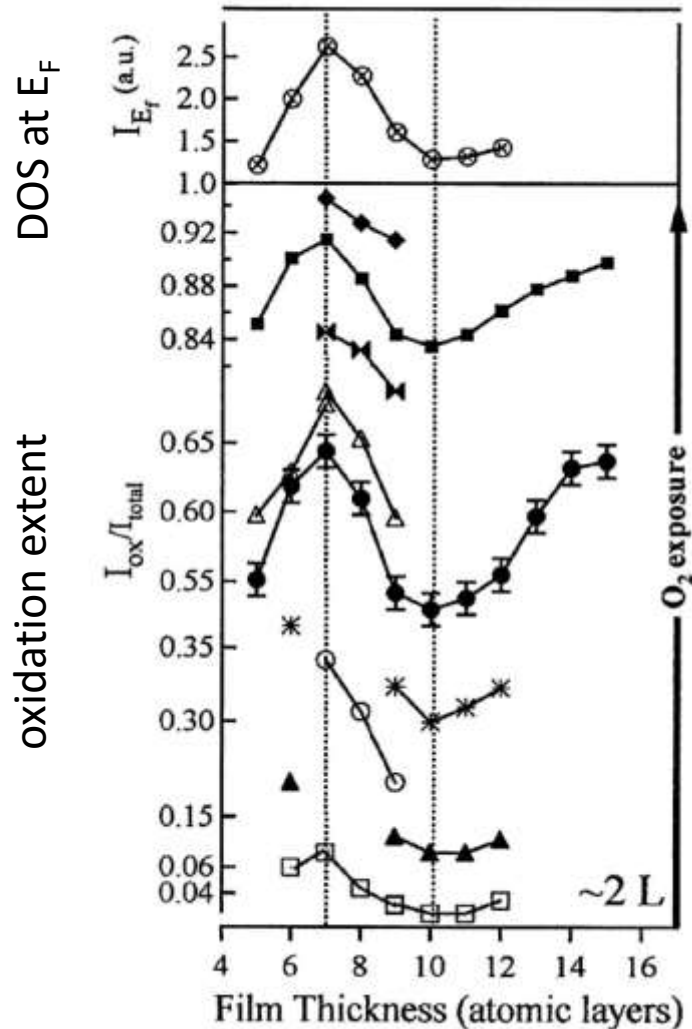


1 μm

\downarrow O_2 exposure



L. Aballe *et al.*, Phys. Rev. Lett. **93**, 196103 (2004)



FACTS

- ✓ Strong variations in the oxidation extent are correlated to thickness and to the density of states at E_F
- ✓ XPEEM is a powerful technique for correlating chemistry and electronic structure information

SIGNIFICANCE OF THE EXPERIMENTS

- ✓ Control on film thickness enables modifying the molecule-surface interaction
- ✓ Theoretical explanation: Decay length of QWS into vacuum is critical: it reproduces peak of reactivity in experimental data. See Binggeli and M. Altarelli, Phys.Rev.Lett. 96, 036805 (2005)

L. Aballe *et al.*, Phys. Rev. Lett. 93, 196103 (2004)

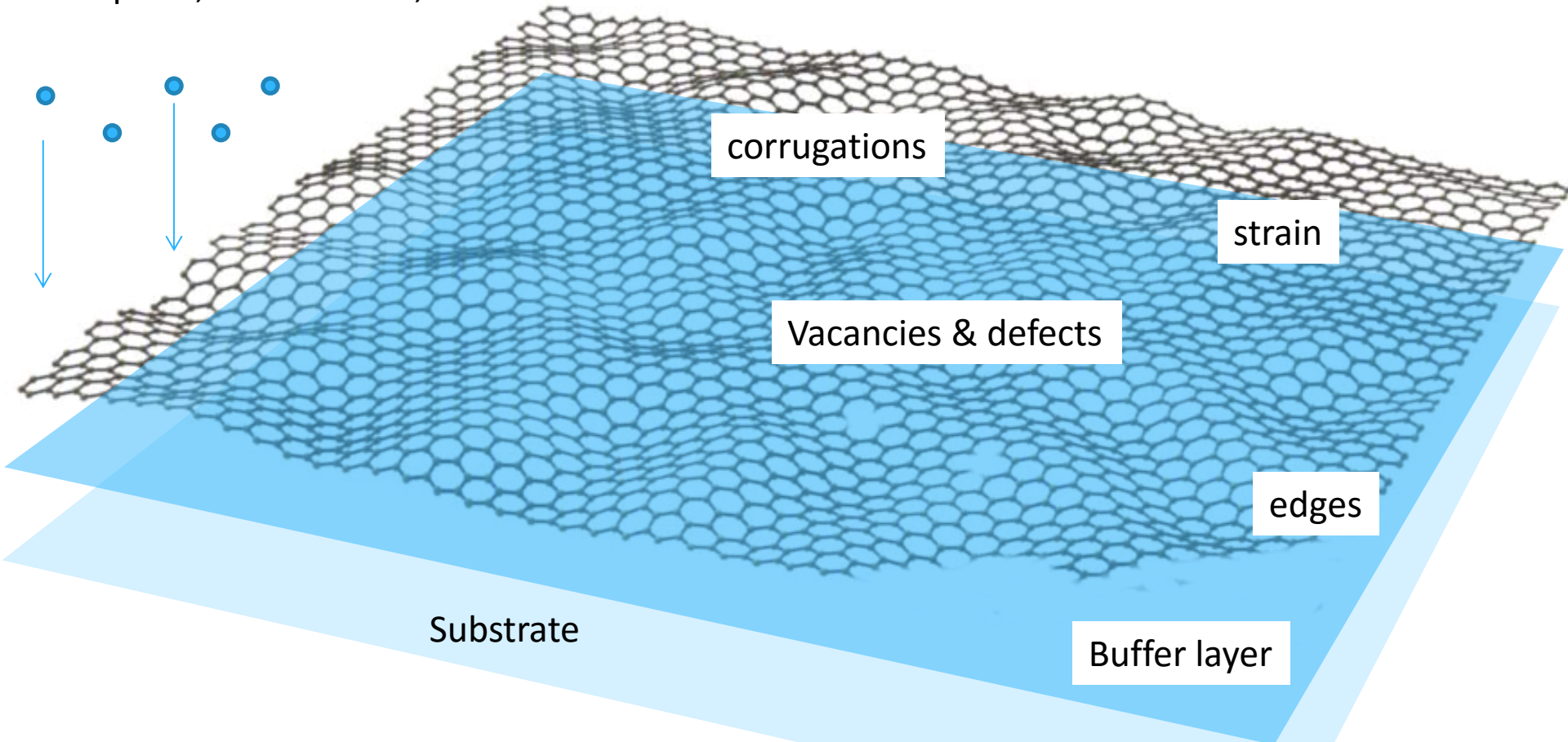
XPEEM studies of the metal-graphene interface



Elettra Sincrotrone Trieste

adsorption, intercalation,

Irradiation, functionalization, implantation



- Understand and control the fundamental interactions occurring at the interface
- **verify the properties (crystal quality, stoichiometry, electronic structure) at the mesoscale!**

High temperature graphene growth on Ir(100)



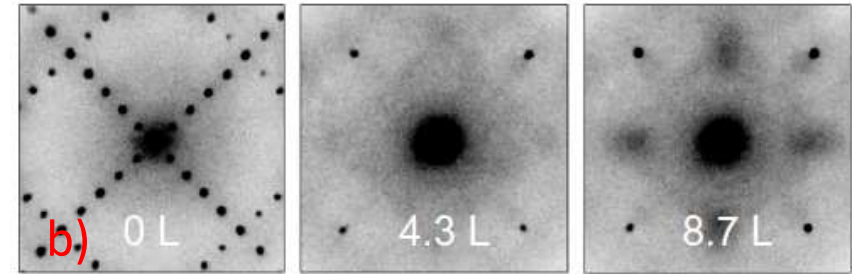
Elettra Sincrotrone Trieste

LEEM imaging

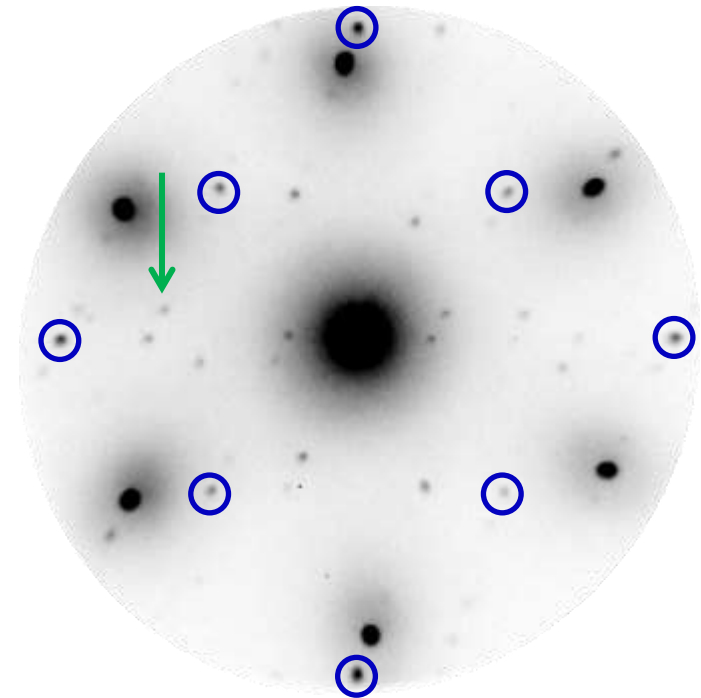


$T > 800 \text{ C}; P = 2 \cdot 10^{-8} \text{ mbar ethylene}$

microprobe-LEED: Ir



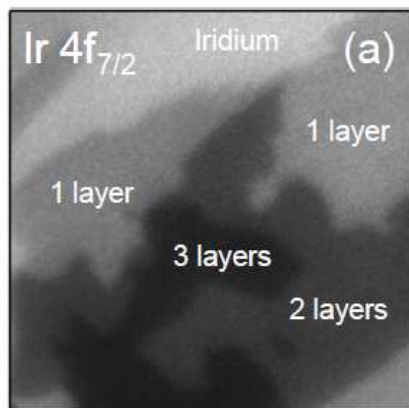
microprobe-LEED: graphene



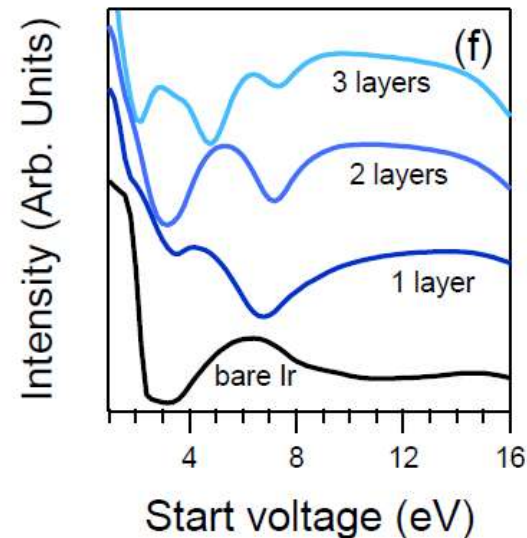
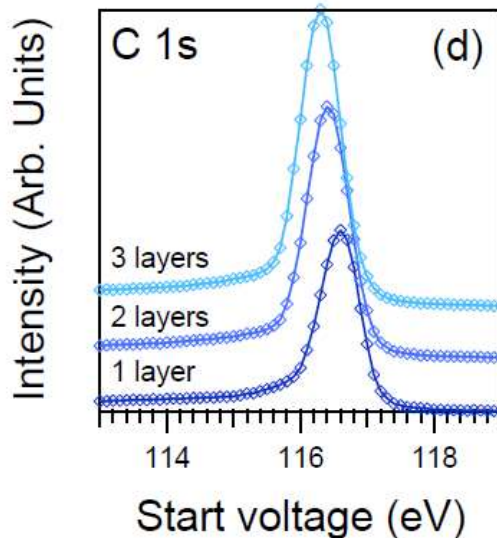
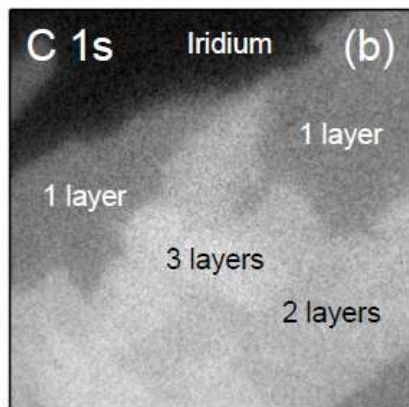
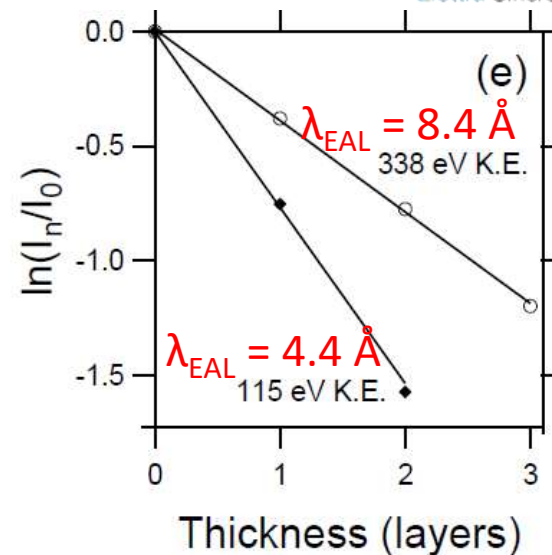
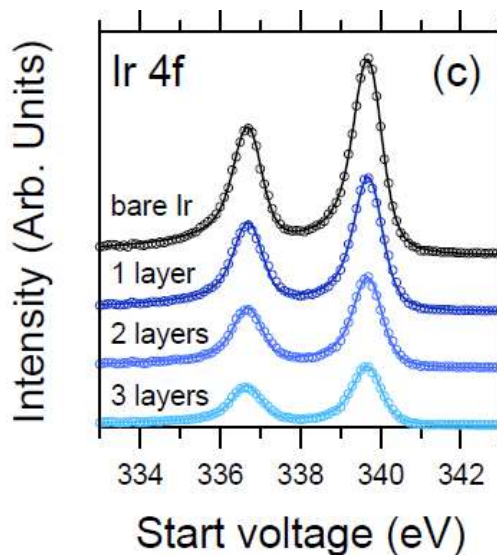
Graphene thickness determination



Elettra Sincrotrone Trieste



1 μm



Growth on Ir(100) at 760°C:
formation of multilayers

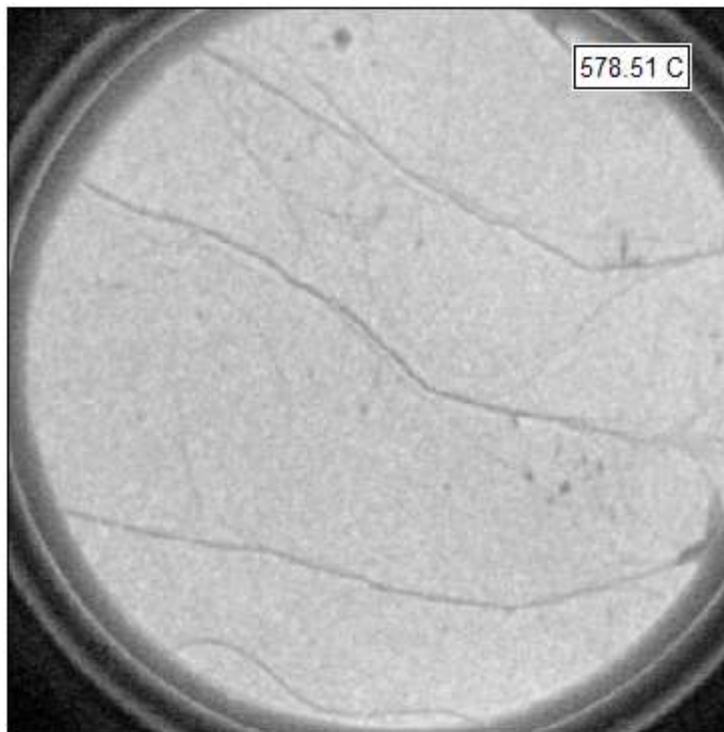
Reversible graphene phase transformation



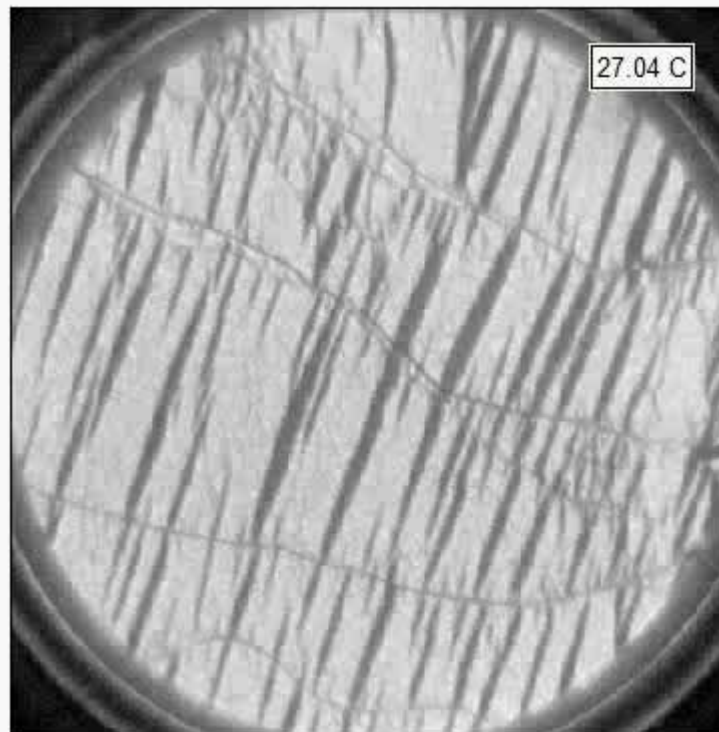
Elettra Sincrotrone Trieste

Upon cooling a new graphene phase nucleates (dark stripes)

The stripes disappear upon annealing to high temperature.



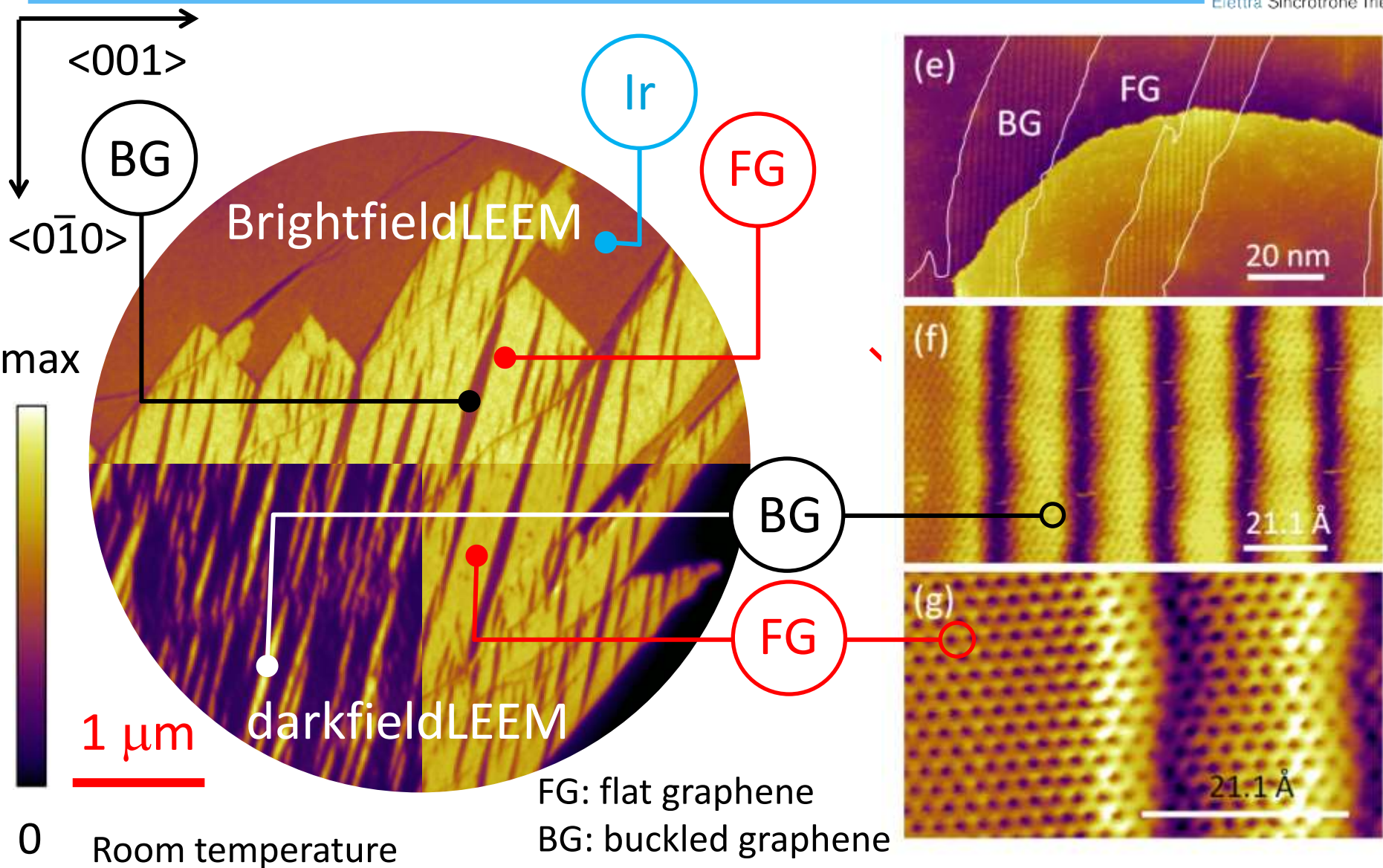
1 μm



1 μm

LEEM, Fov 4 μm , S.V. 13 eV

Graphene/Ir(100): structure of FG and BG



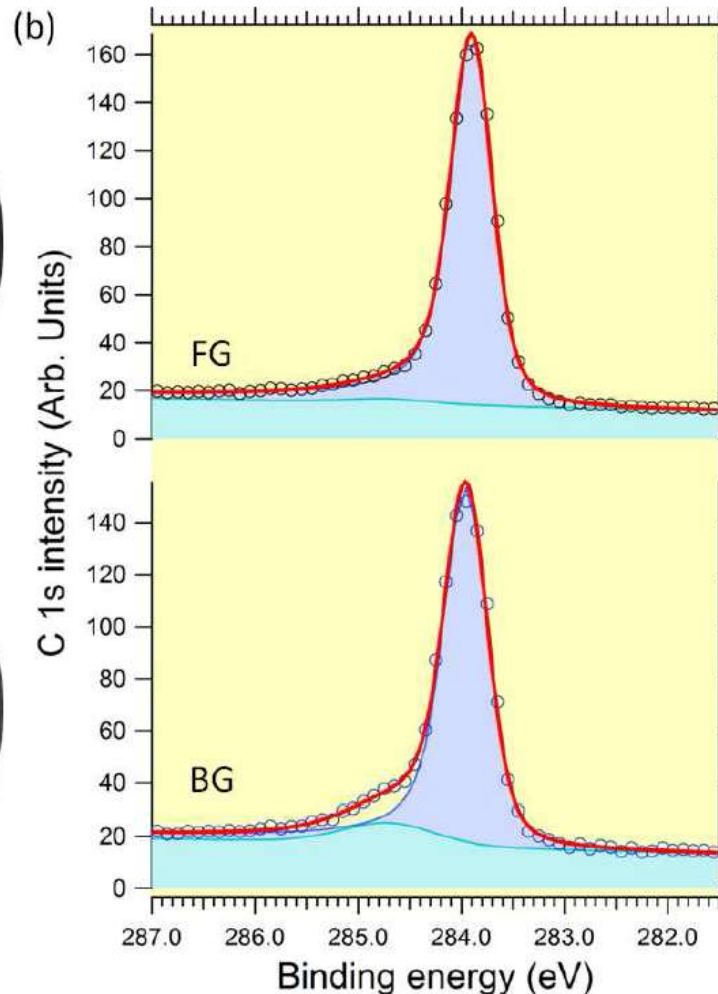
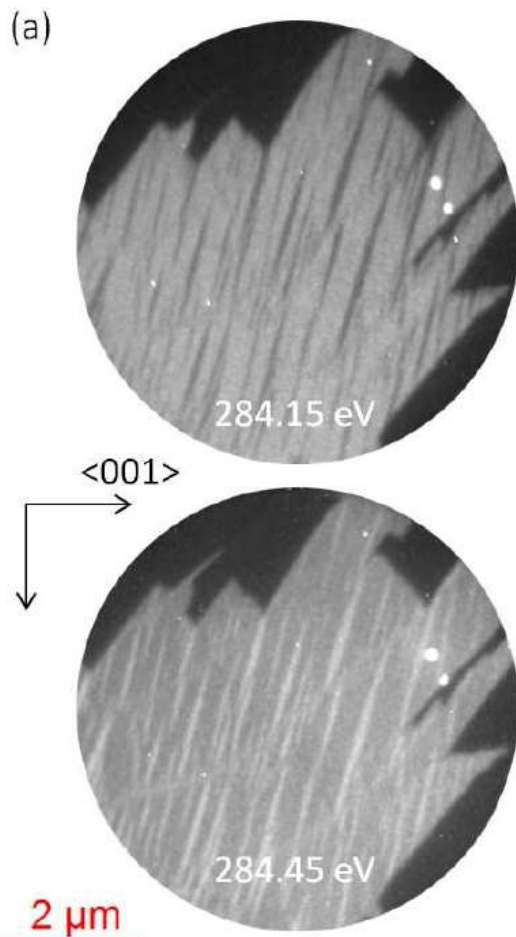
Buckled graphene unit cell by ab-initio



Elettra Sincrotrone Trieste

buckled graphene unit cell

Buckled Graphene



Exceptionally large buckling

GGA:

- ❖ Min Ir-C distance of 1.9 Å
- ❖ Max Ir-C distance of 4.0 Å

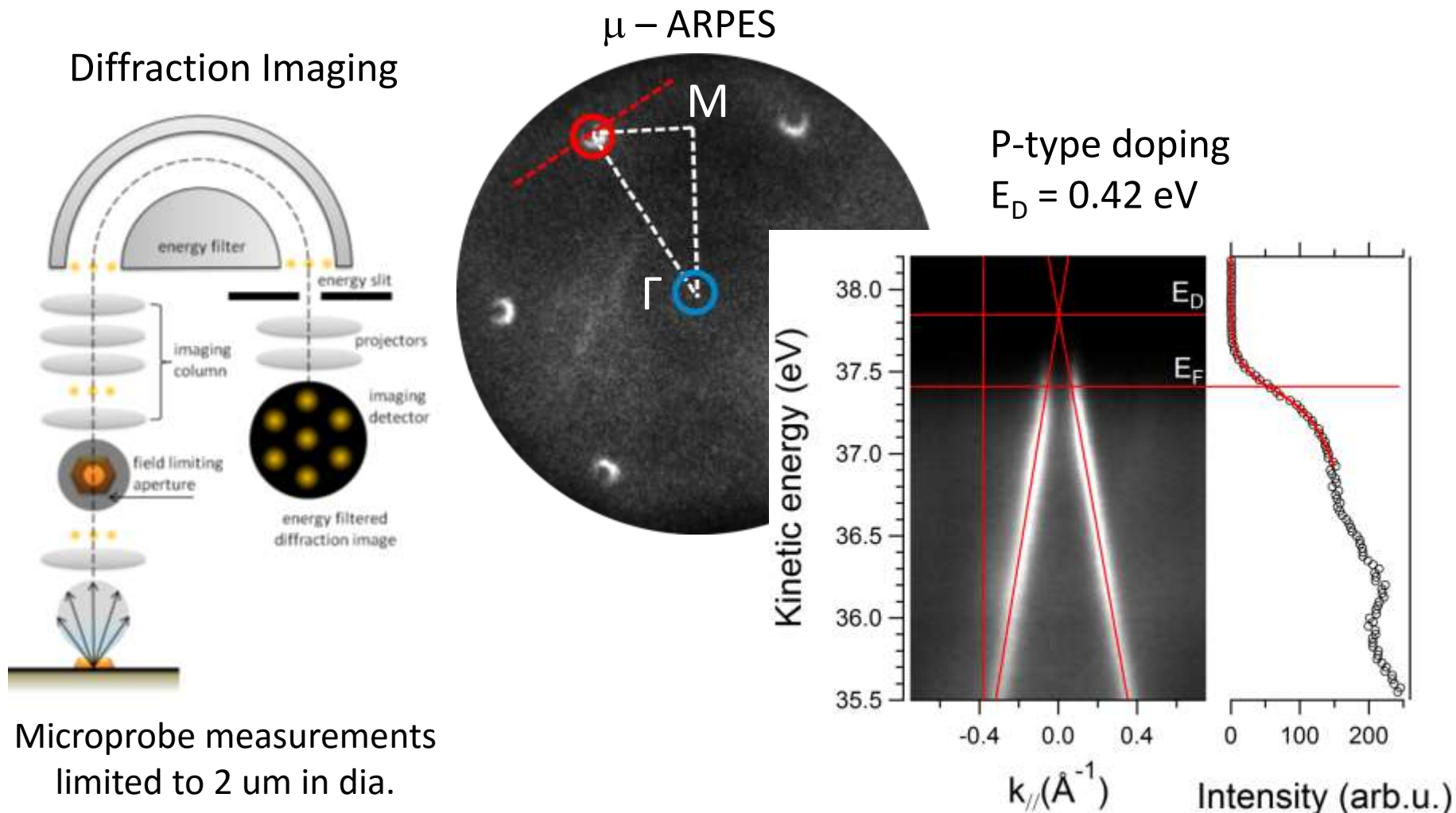
DFT-D:

- ❖ Min Ir-C distance of 2.1 Å
- ❖ Max Ir-C distance of 3.7 Å
- ❖ 18 atoms over 160 (i.e. 11%) are **chemisorbed**, the others are physisorbed

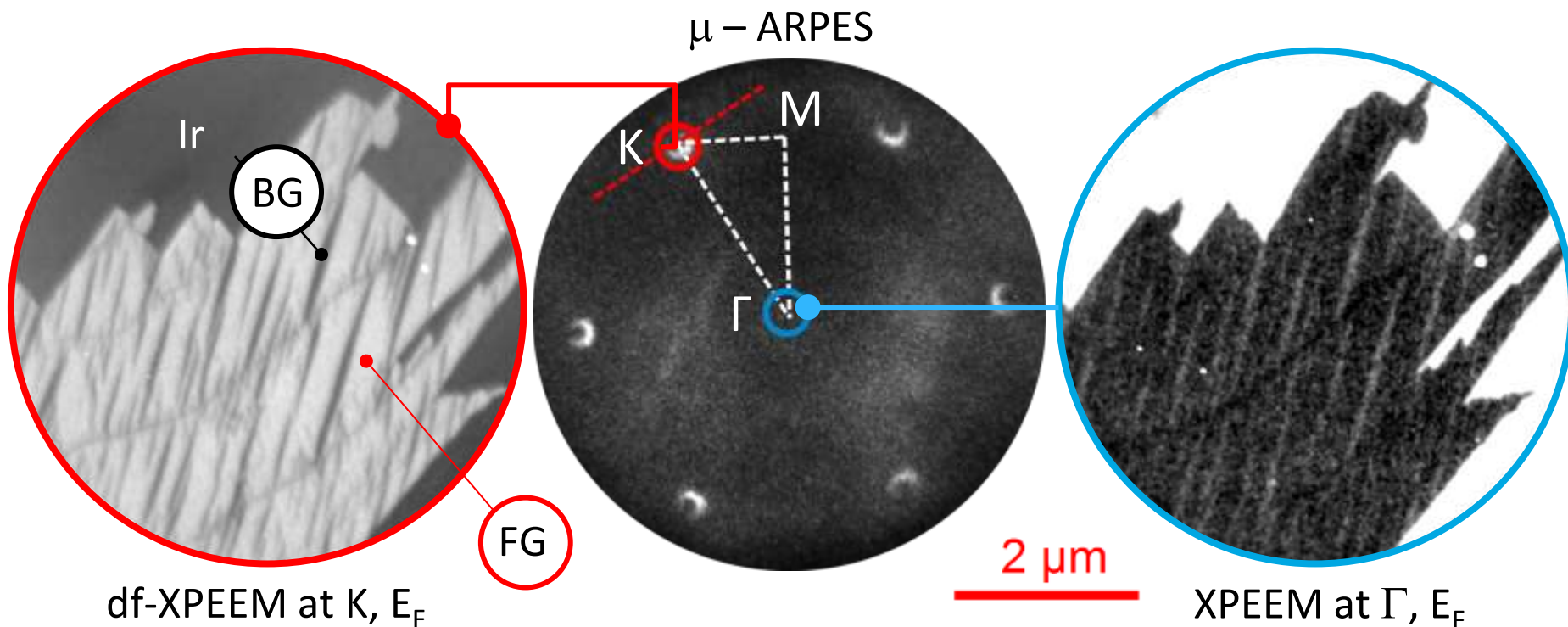
Ab-initio calculations by N. Stojic, N. Binggeli, ICTP;

Buckled graphene shows regular one-dimensional ripples with periodicity of 2.1nm.

microprobe diffraction cannot resolve FG and BG!

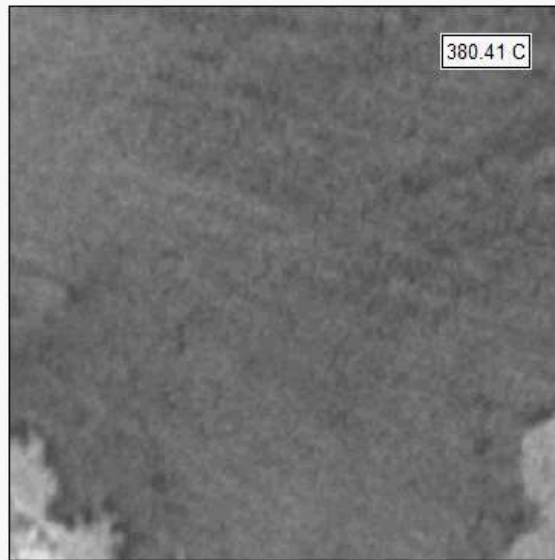


Issues: what is the difference in electronic structure between FG and BG?
do they both show the same Dirac-like dispersion?



- ❖ emission from the π band at K allows quantifying local DOS of FG and BG phases.
- ❖ DF-PEEM images at E_F clearly indicate that **only FG** shows high DOS at K.
- ❖ much reduced DOS and contrast inversion at $\Gamma \rightarrow$ BG hybridization and metallicity.
- ❖ Microprobe-ARPES data are thus representative of the FG phase, not the BG one!

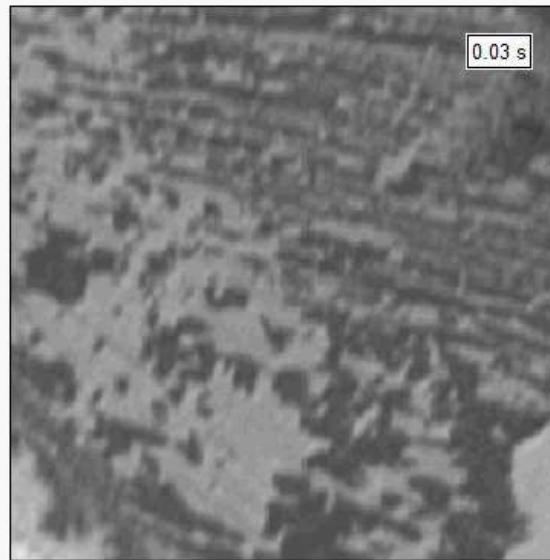
1: carbide nucleation



1 μm

The Ni-carbide nucleates under rotated graphene, $T < 340^{\circ}\text{C}$
Patera et al., ACS Nano 7, 7901 (2013)

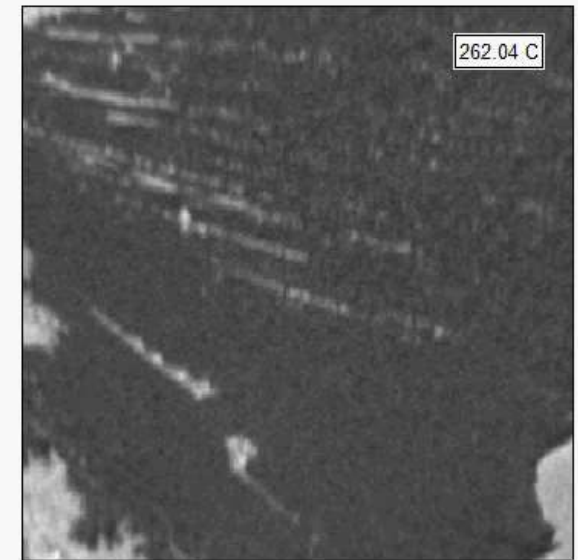
2: carbide growth



1 μm

A uniform layer of Ni-carbide is formed below graphene in about two hours

3: carbide growth



1 μm

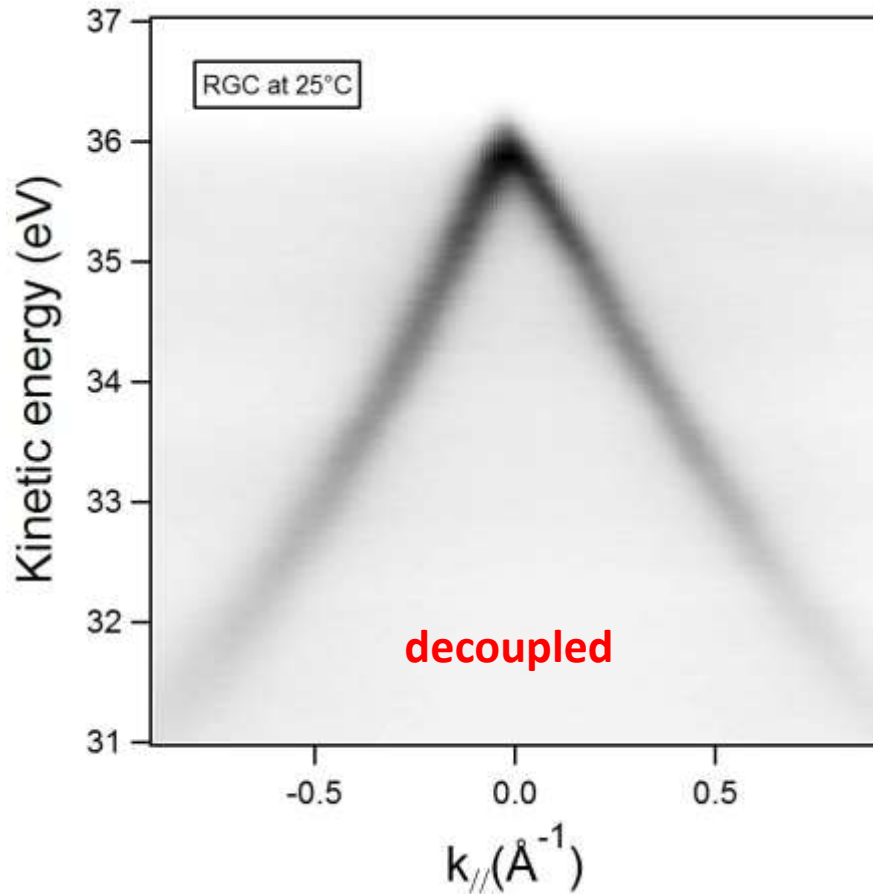
The carbide is dissolved into the bulk at about 360°C . The process is repeatable!

All movies: LEEM FoV 6 μm, electron energy: 11 eV

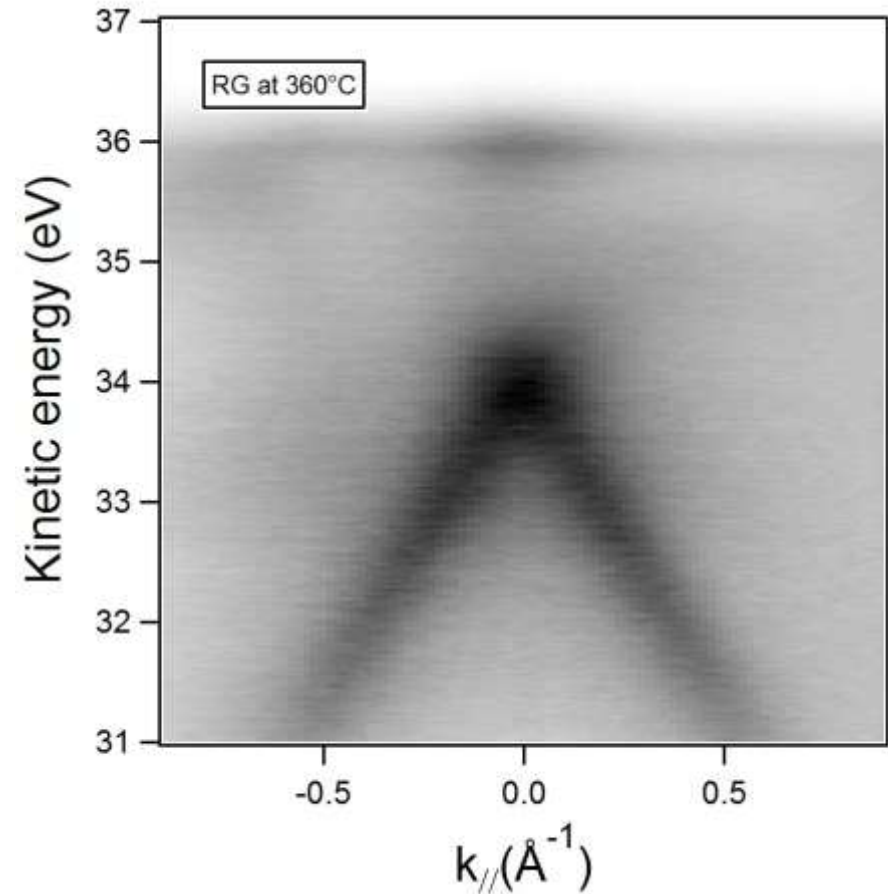
Electronic structure is by μ -ARPES



Elettra Sincrotrone Trieste



Rotated graphene with Ni-carbide underneath at room temperature;
There's no double layer

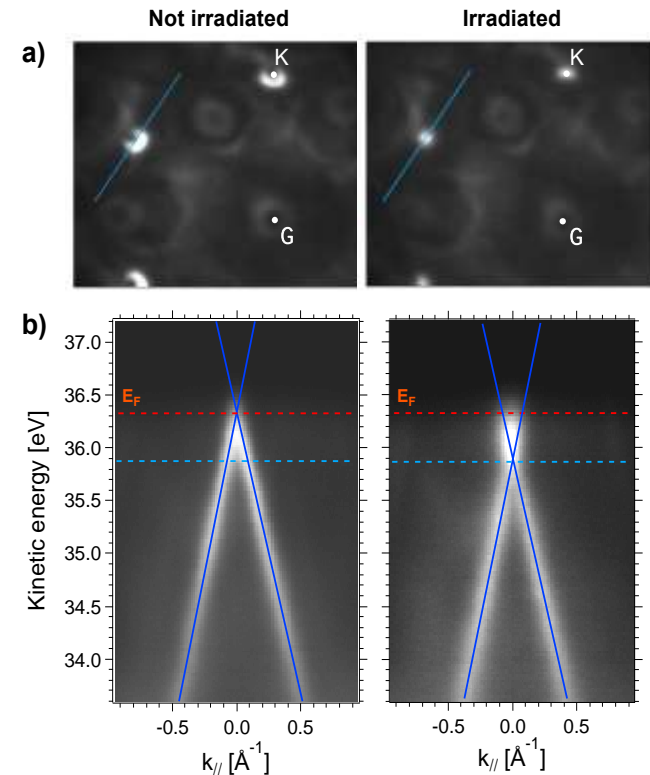
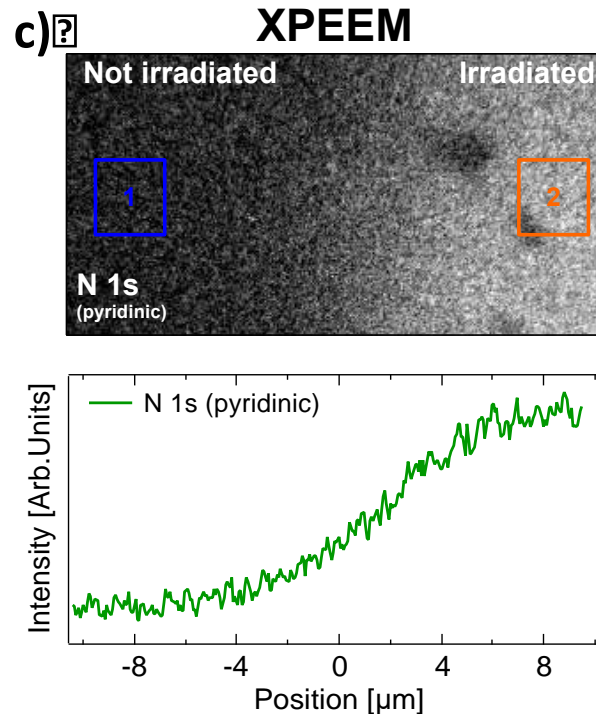
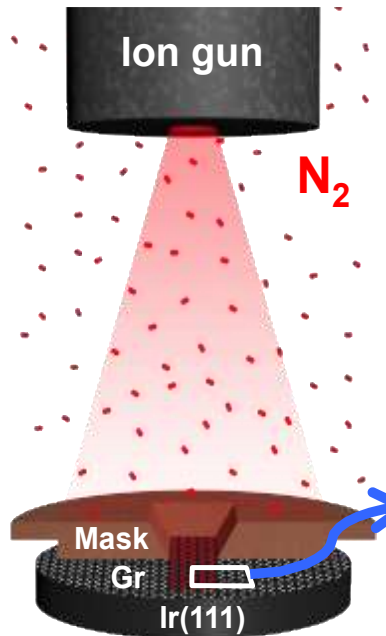


Rotated graphene without Ni-carbide underneath at 365°C

Ion irradiation of graphene:

- **Substitutional implantation:**
 - Local doping by low energy ion irradiation
- **Ar nanobubbles ripening under graphene**
 - Strain engineering! [C. Lee et al., Science 321, 385 (2008)]
 - Anvil cells (high pressure) [Xuan Lim et al., Nat. Comm. 4, 1556 (2013)]
 - Exhotic magnetic properties [N. Levy et al. Science 329, 544 (2010)]

2D heterojunction by low energy N_2^+ irradiation

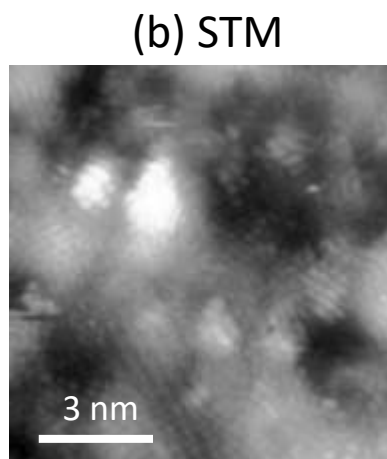
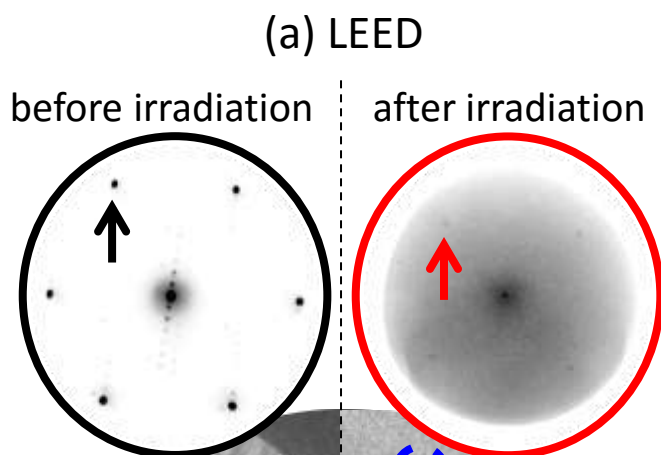


- ❖ Small damage to graphene lattice;
- ❖ Thermal stability: graphitic: stable above 700°C; pyridinic stable up to 400°C;
- ❖ Boundary also stable upon annealing (no migration/loss)
- ❖ Negative doping \rightarrow formation of doping patterns

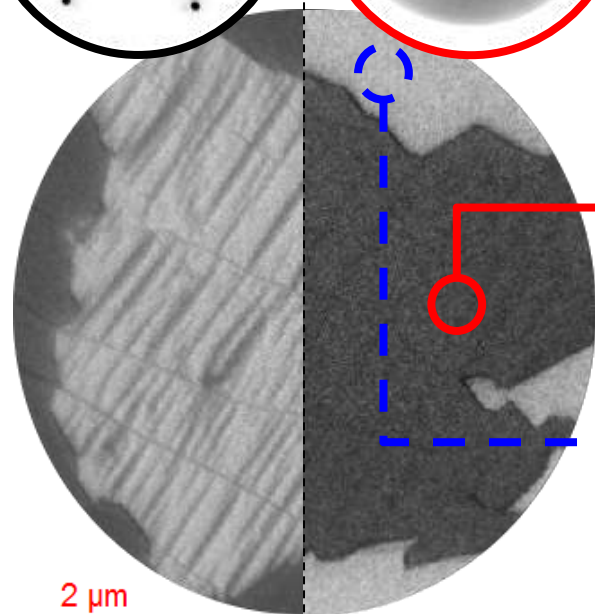
Morphology of Ar⁺ irradiated graphene/Ir(100)



Elettra Sincrotrone Trieste

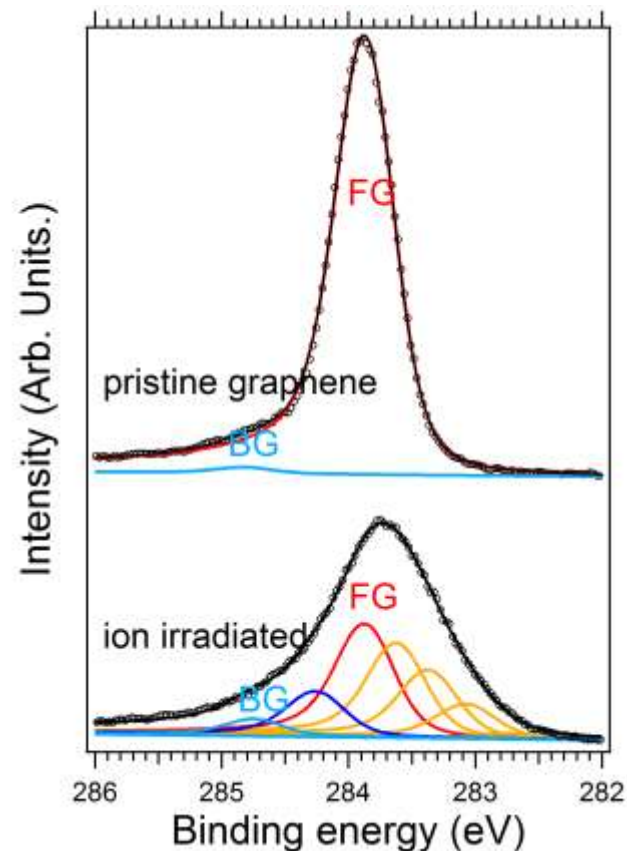
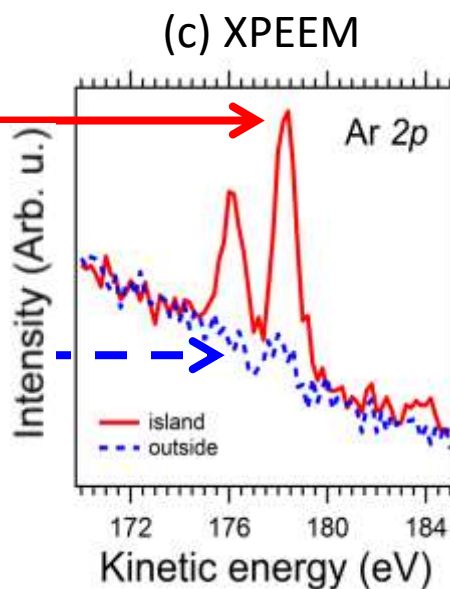


Rough morphology, but ...
graphene is continuous
average height 0.15 nm!



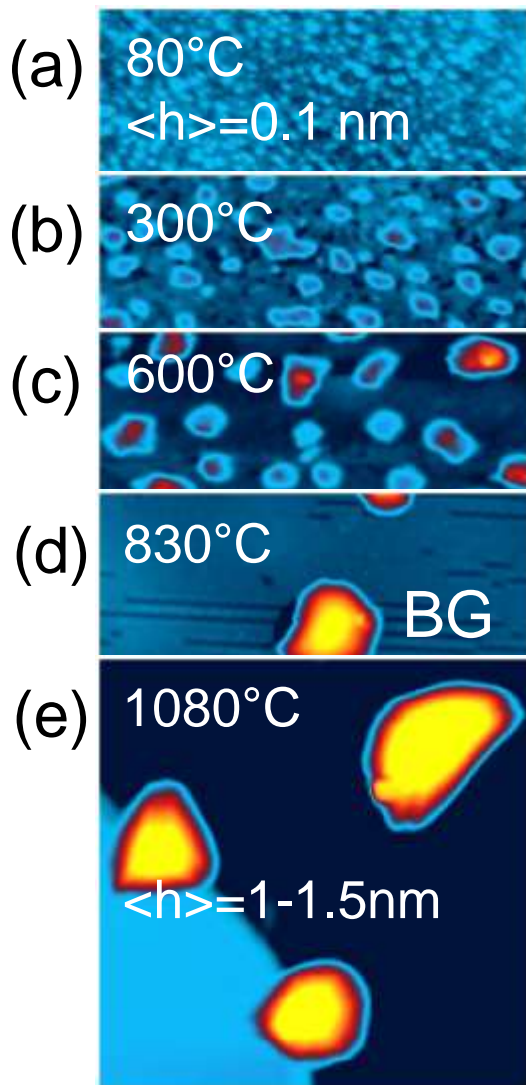
LEEM 12 eV

Irradiation with 0.5keV Ar⁺ 7 s

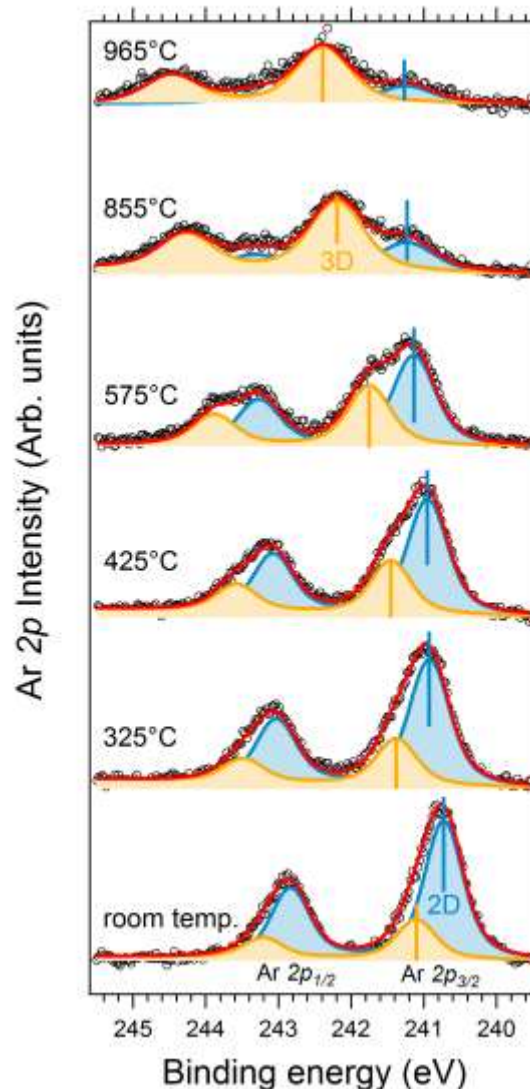


Evolution upon annealing: STM and μ -XPS

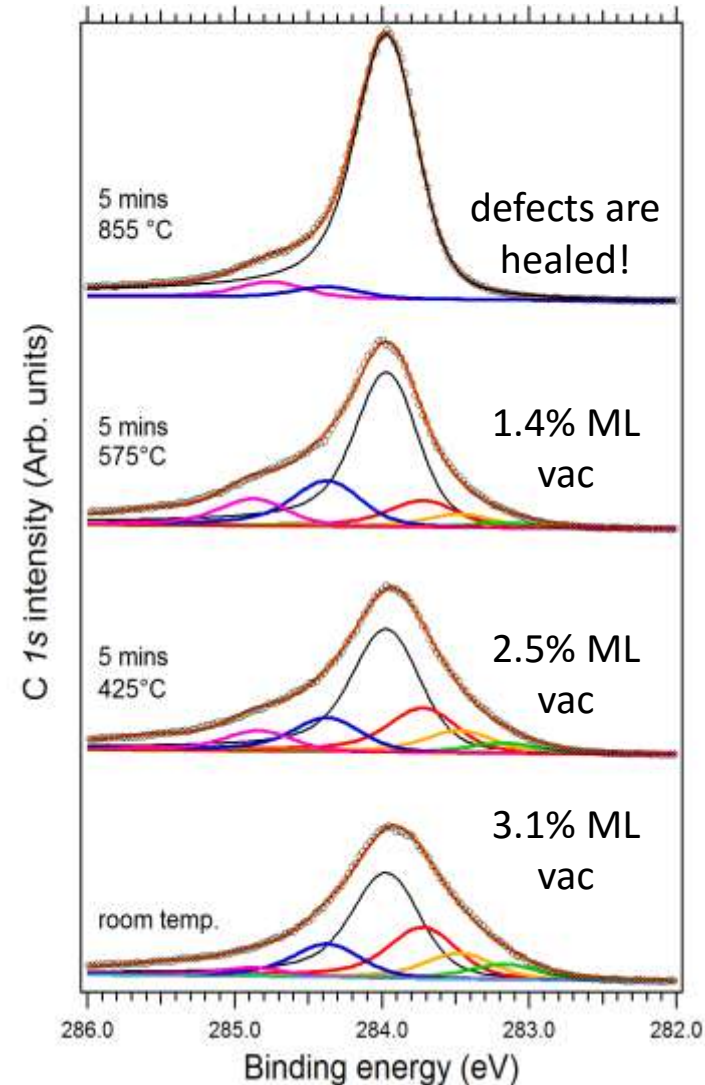
STM



Ar 2p



C 1s

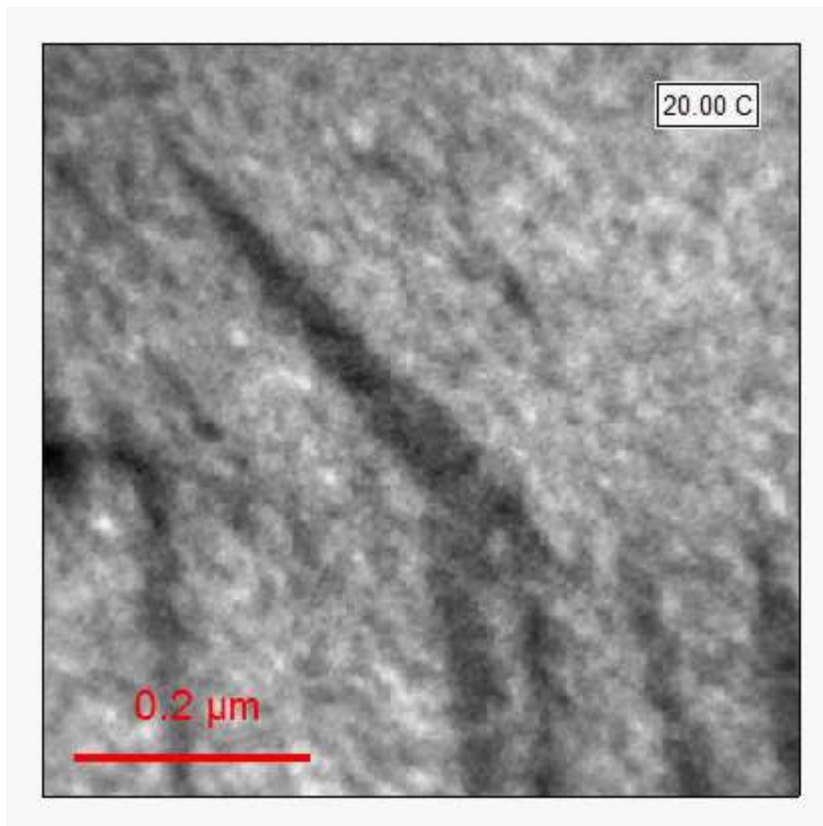


LEEM & XPEEM formation of Ar nanobubbles

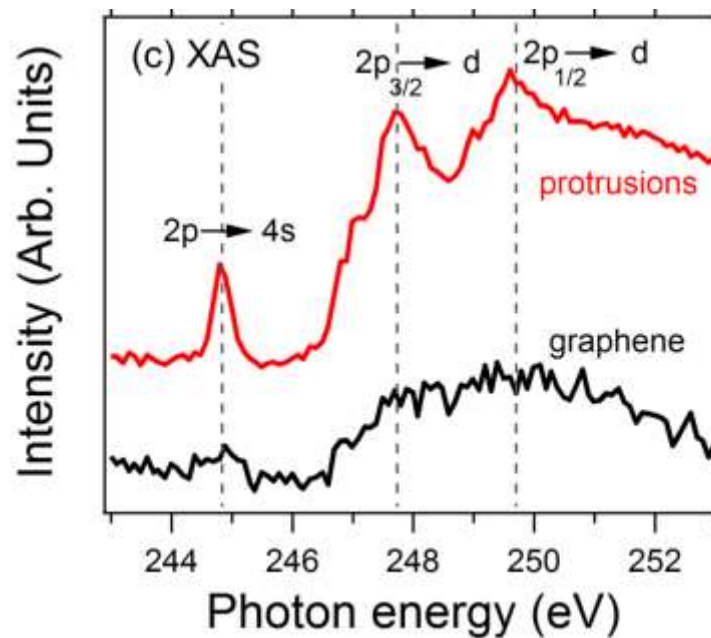
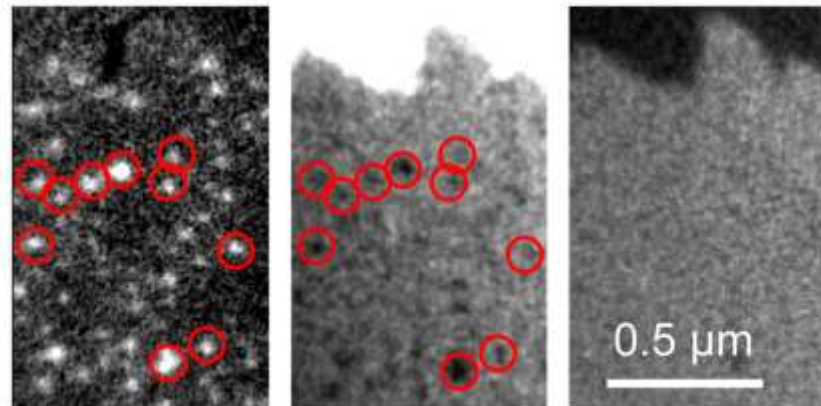


Elettra Sincrotrone Trieste

LEEM movie 12 eV



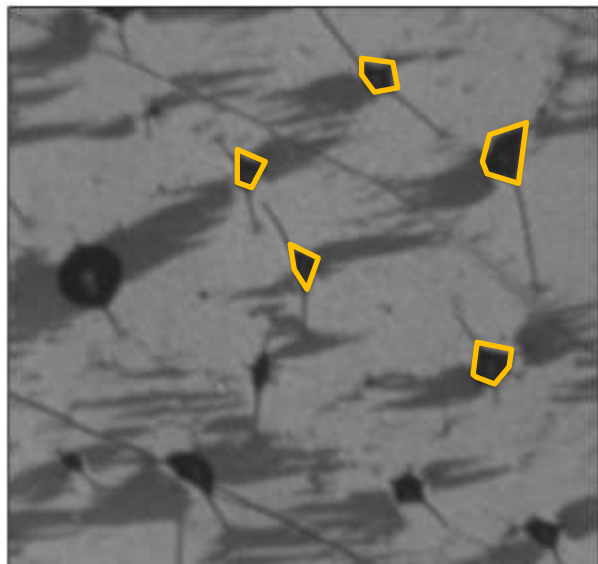
(d) XAS Ar L₃ (e) XPEEM Ir 4f_{7/2} (f) XPEEM C1s



NB formation for g/Ne/Ir(100)

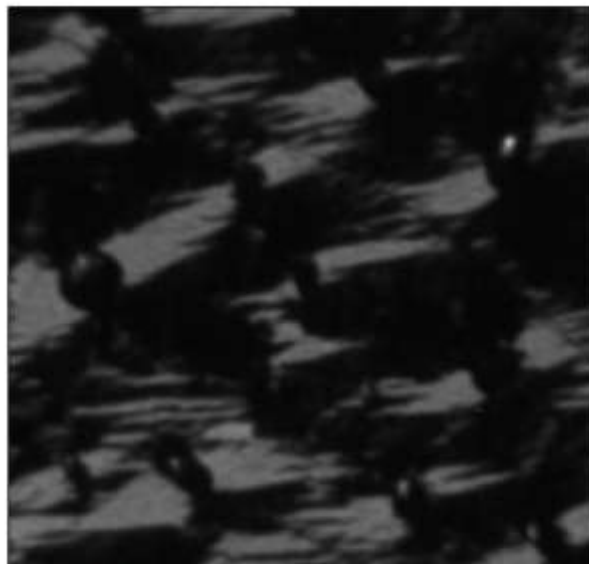
100 eV Ne⁺ ion irradiation was followed by 5 min annealing to 650 °C and subsequent cooling to RT

bright-field LEEM 12 eV



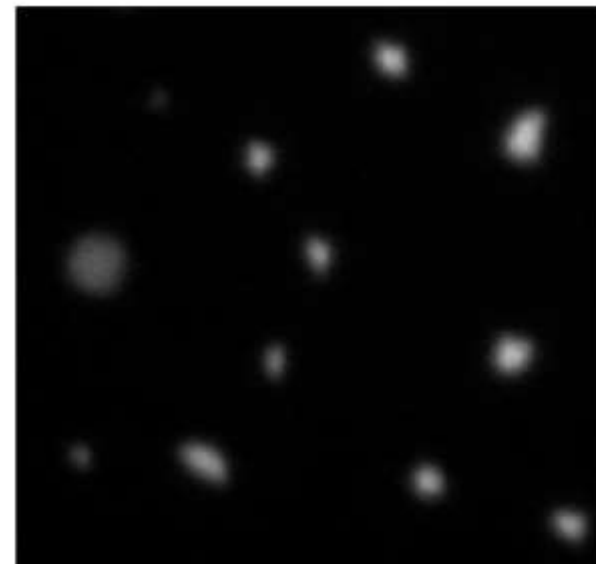
0.5 μm

dark-field LEEM BG phase



0.5 μm

XPEEM imaging Ne 2p



0.5 μm

- Wrinkles surround the larger particles
- At RT, bubbles have a polygonal shape → solid?

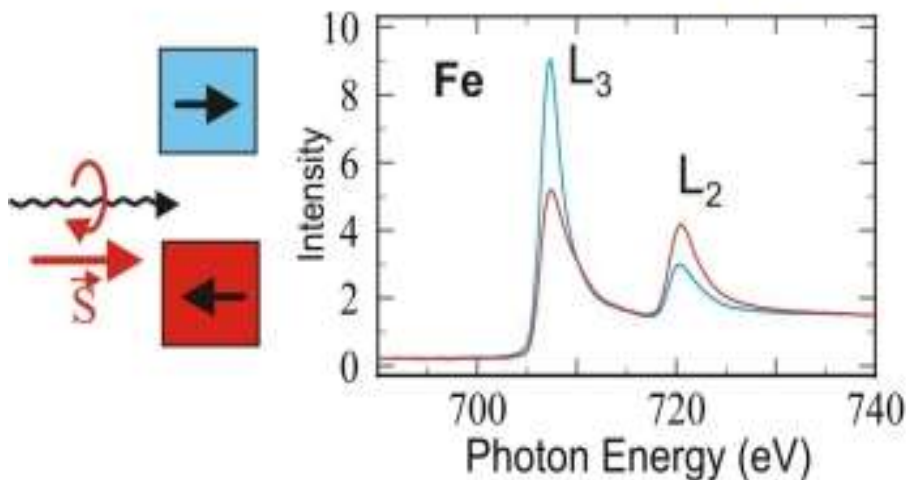
- elemental composition below graphene!
- XPS from individual particles
- Shift to high BE for large clusters



Magnetic imaging

XMCD and XMLD PEEM

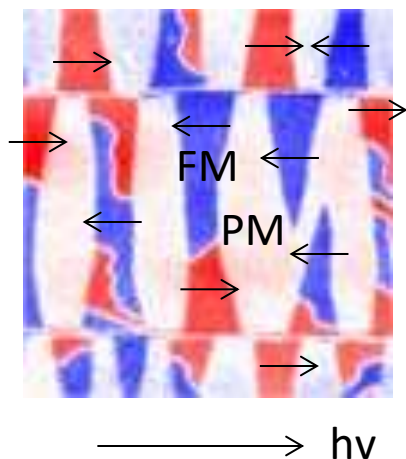
Circular Dichroism - Ferromagnets



X-ray magnetic circular dichroism (XMCD) is the dependence of x-ray absorption on the relative orientation of the local magnetization and the polarization vector of the circularly polarized light

- ✓ Element sensitive technique
- ✓ Secondary imaging with PEEM determine large probing depth (10 nm), buried interfaces.

MnAs/GaAs



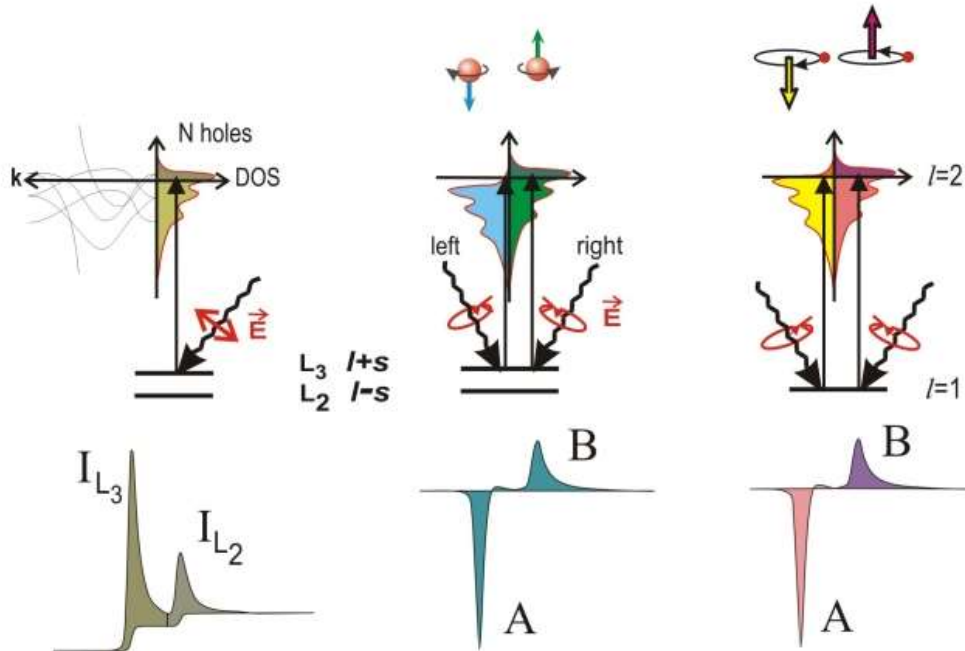
Magnetic domain imaging

At resonance, the secondary electron yield is proportional to the dot product between the magnetization direction and the photon helicity vector, which is parallel or anti-parallel to the beam propagation direction

(a) d-Orbital Occupation

(b) Spin Moment

(c) Orbital Moment

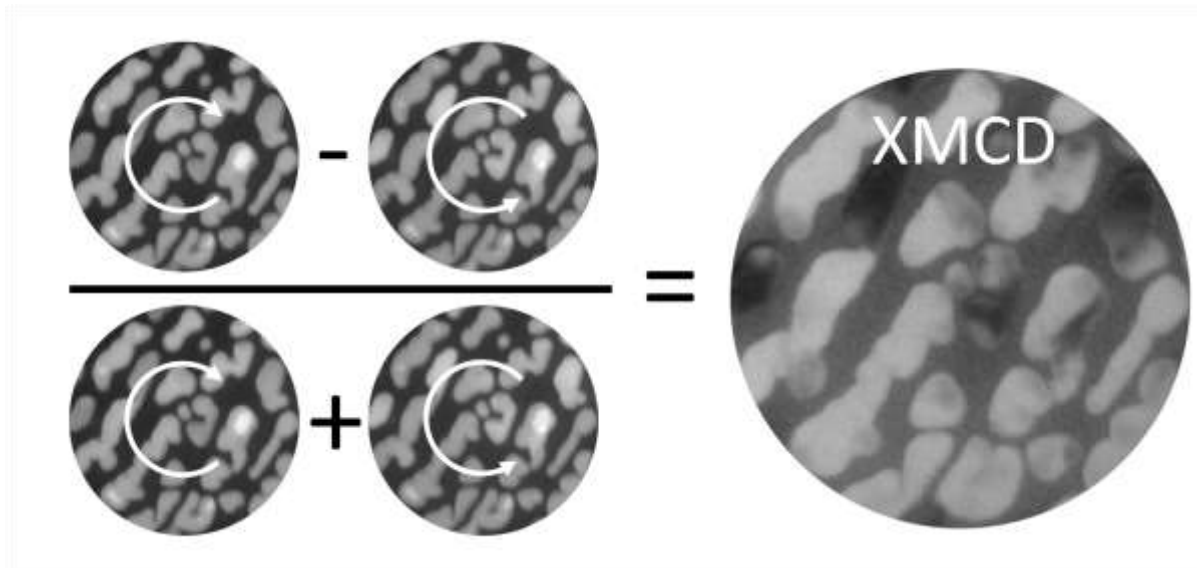


- We **PROBE** 3d elements by exciting 2p into unfilled 3d states
- Dominant channel: $2p \rightarrow 3d$
- White line intensity of the L3 and L2 resonances with the number N of empty d states (holes).

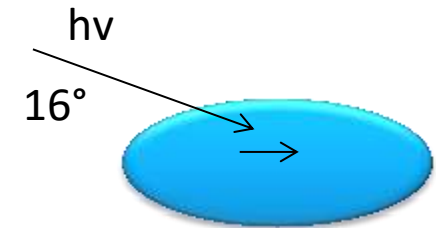
- By using circularly polarized radiation, the angular momentum of the photon can be transferred in part to the spin through the spin-orbit coupling. Photoelectrons with opposite spins are created in the cases of left and right handed polarization. Spin polarization is opposite also for $p_{3/2}$ (L_3) and $p_{1/2}$ (L_2) levels.
- The spin-split valence shell is thus a detector for the spin of the excited photoelectron. The size of the dichroism effect scales like $\cos\theta$, where θ is the angle between the photon spin and the magnetization direction.
- **Refs: IBM. J. Res. Develop. 42, 73 (1998) and J. Magn. Magn. Mater. 200, 470 (1999).**

XMCD image algebra

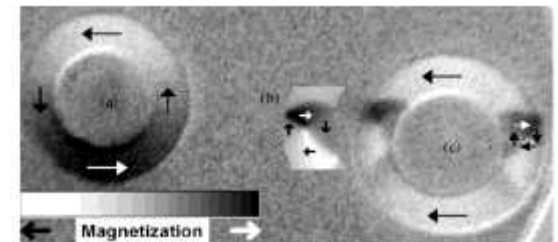
The size of the dichroism effect scales like $\cos\theta$, where θ is the angle between the photon spin and the magnetization direction. Hence the maximum dichroism effect (typically 20%) is observed if the photon spin and the magnetization directions are parallel and anti-parallel. Sum rules allows measuring orbital and spin moments



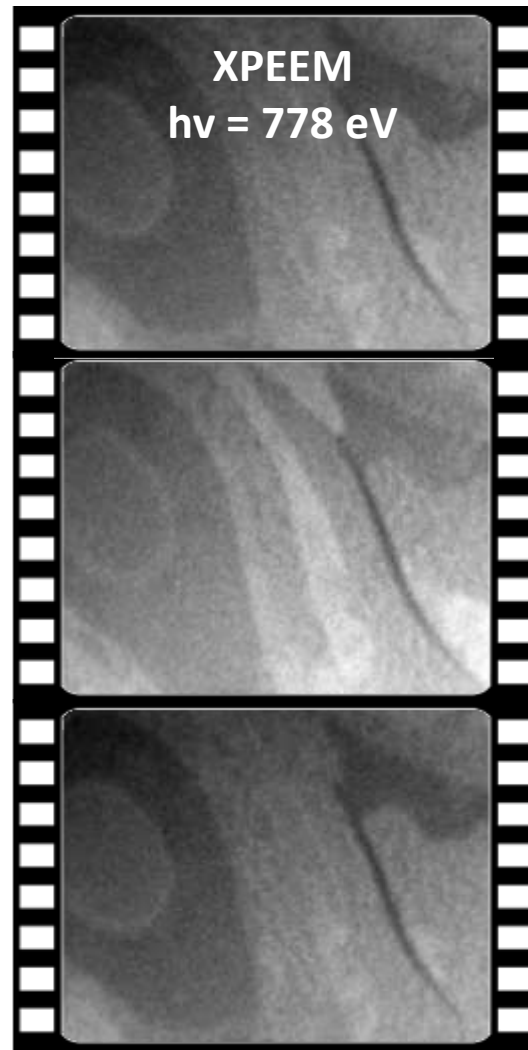
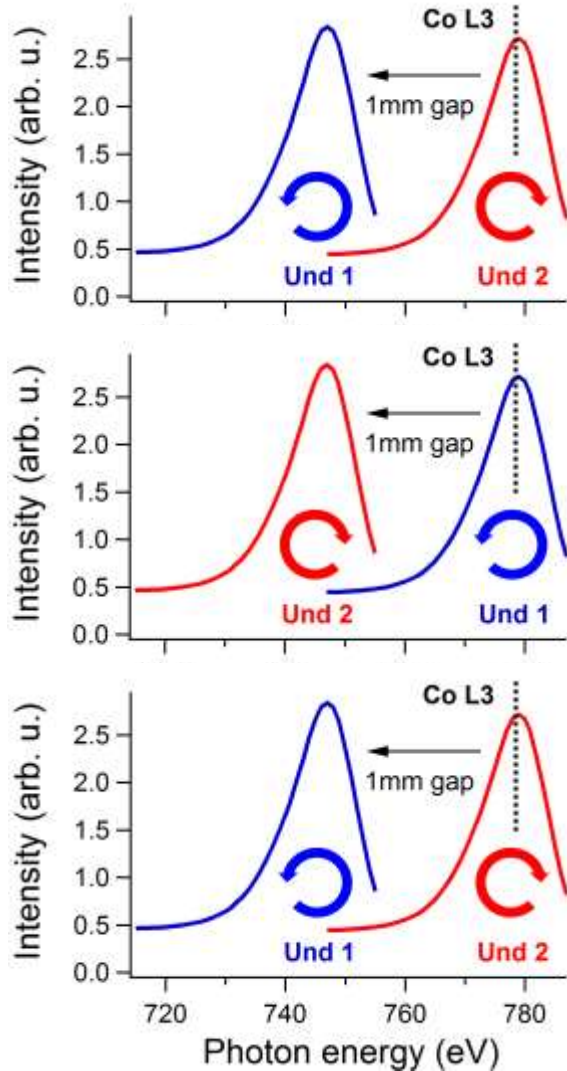
Geometry



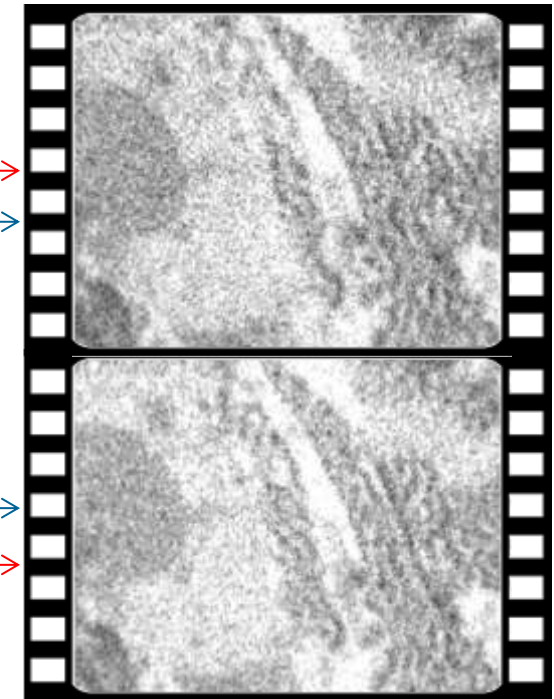
the illumination geometry,
 \rightarrow *in plane* component of
M



Beamline settings



$$I^{XMCD} = \frac{I^- - I^+}{I^- + I^+}$$

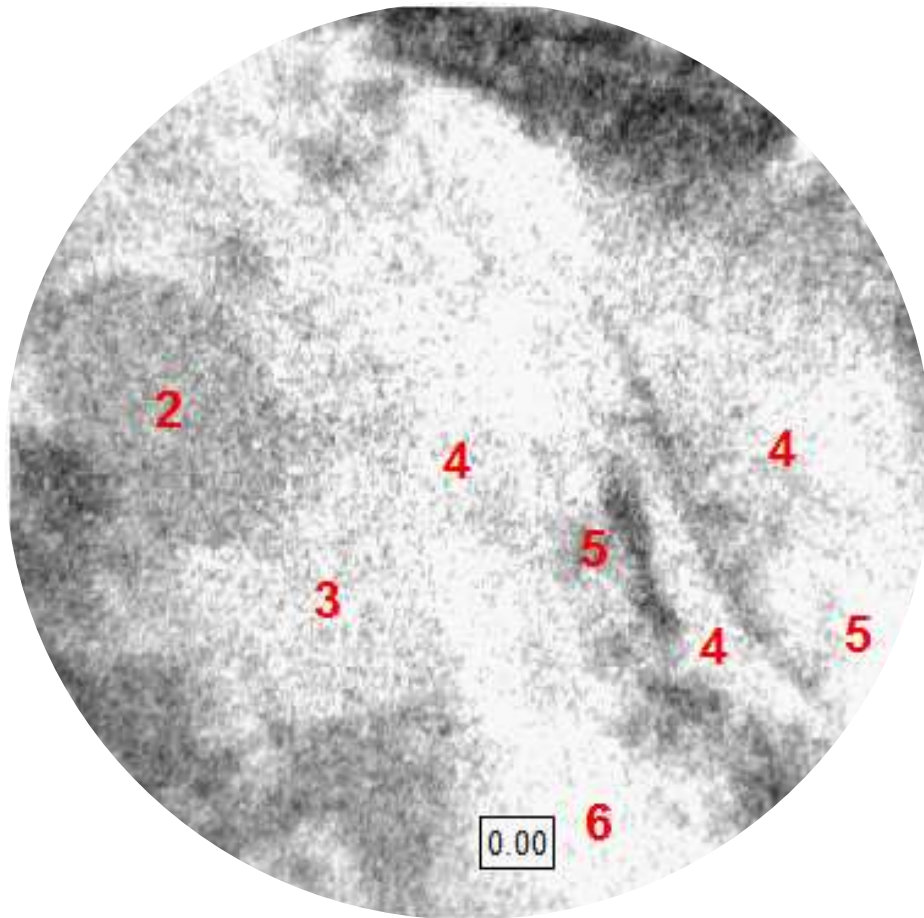


Time resolution about 25 s

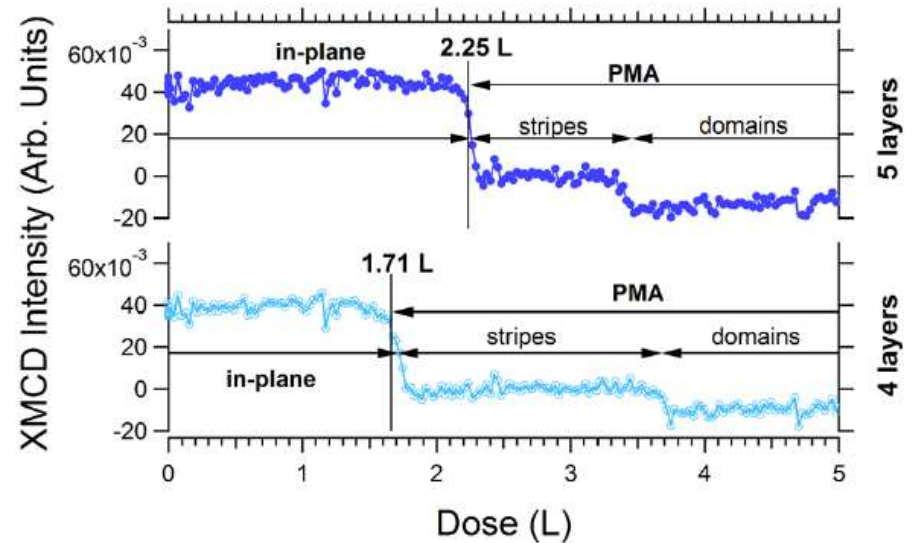
FoV 6 μm ; 12 sec/frame

XMCD movie of a spin reorientation transition

XMCD movie @ Co L_3 edge in $P_{CO}=2 \cdot 10^{-9}$ mbar; frame acquisition 12 s, FoV $6 \mu\text{m}$



4 atomic layers Co more reactive than 5 & 3



Different layers have different period
Unstable domain structure
Period changes with CO dose

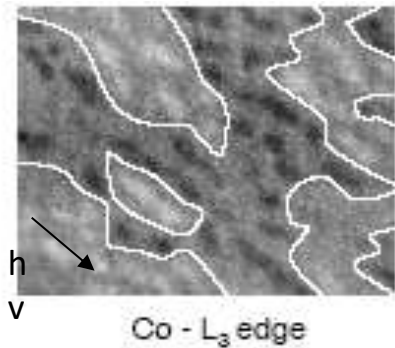
Examples of XMCD-PEEM applications



Elettra Sincrotrone Trieste

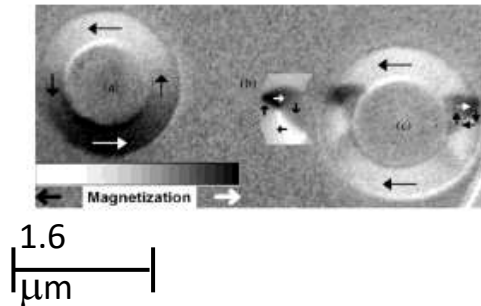
MAGNETIC STATE using XMCD & XMLD

Co nanodots on Si-Ge

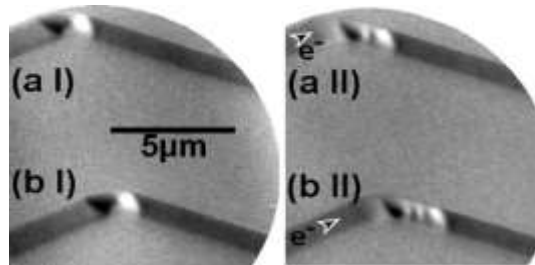


A. Mulders et al,
Phys. Rev. B 71,
214422 (2005).

patterned structures

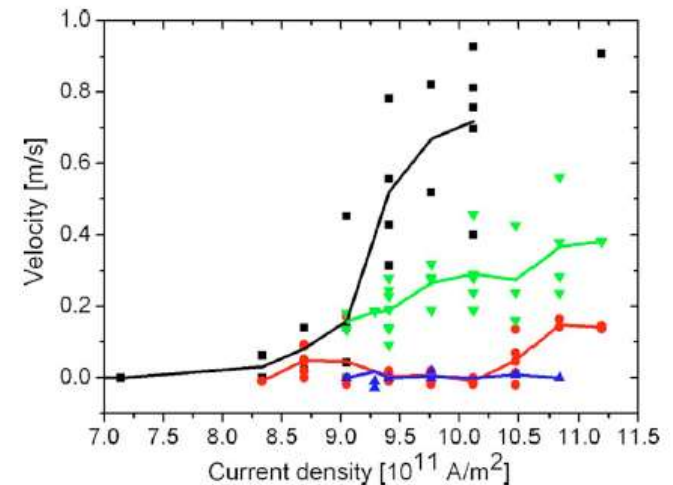


pulse injection



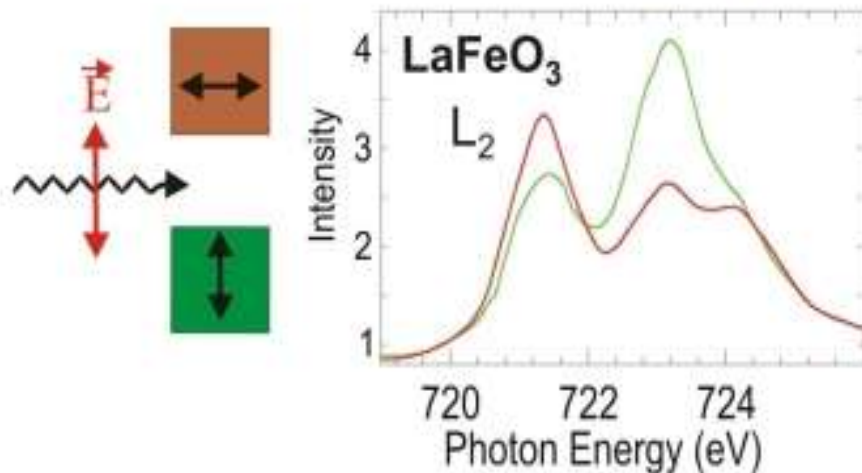
M. Klauui et al,
PRL, PRB 2003 - 2010

domain wall motion induced by spin currents



Laufenberg et al,
APL 88, 232507(2006).

Linear Dichroism - Antiferromagnets



In the presence of spin order the spin-orbit coupling leads to preferential charge order relative to the spin direction, which is exploited to determine the spin axis in antiferromagnetic systems.

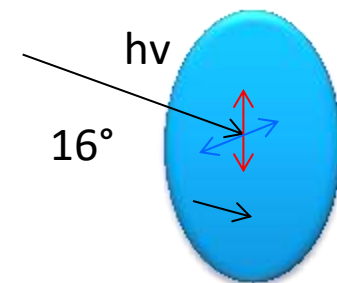
- ✓ Element sensitive technique
- ✓ Secondary imaging with PEEM determine large probing depth (10 nm), buried interfaces.
- ✓ Applied in AFM systems (oxides such as NiO)

Absorption intensity at resonance

$$I(\vartheta, \theta, T) = a + b(3 \cos^2 \vartheta - 1) \langle Q_{zz} \rangle + c(3 \cos^2 \theta - 1) \langle M^2 \rangle_T + d \sum_{i,j} \langle \hat{s}_i \cdot \hat{s}_j \rangle_T$$

1st term: quadrupole moment, i.e. electronic charge (not magnetic!)

2nd term determines XMLD effect; θ is the angle between E and magnetic axis A; XMLD max for E || A;



Linear vertical and linear horizontal polarization of the photon beam

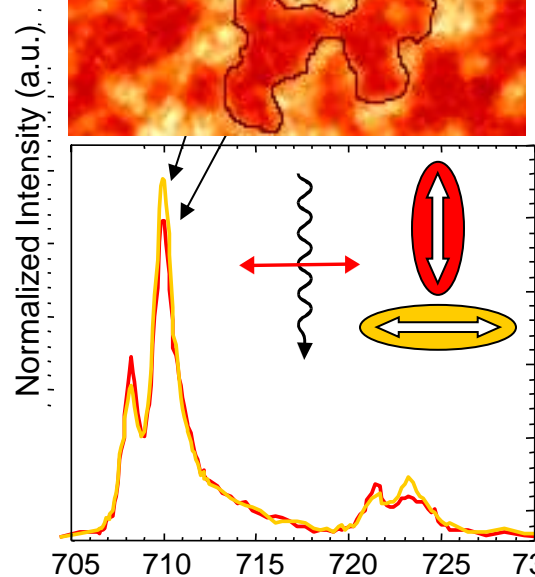
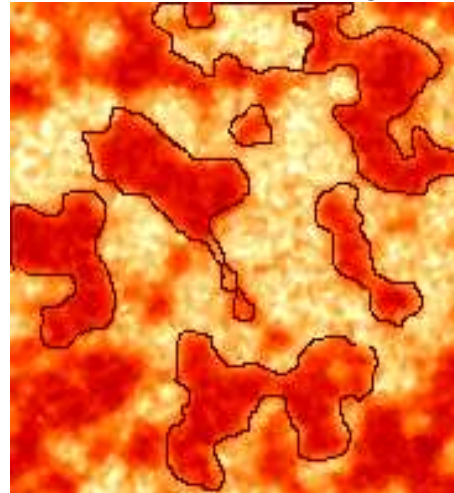
Direct observation of the alignment of ferromagnetic spins by antiferromagnetic spins

F. Nolting⁺, A. Scholl⁺, J. Stöhr[†], J. W. Seo^{‡§}, J. Fompeyrine[§], H. Siegwart[§], J.-P. Locquet[§], S. Anders⁺, J. Lüning[†], E. E. Fullerton[†], M. F. Toney[†], M. R. Scheinfein^{||} & H. A. Padmore⁺

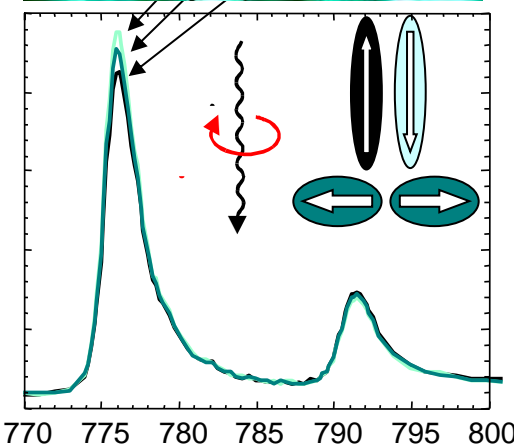
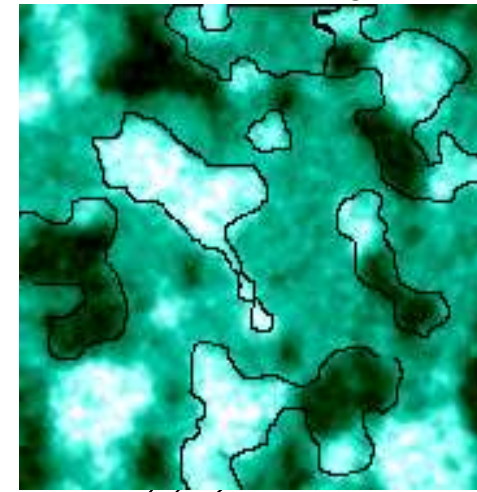
Nature, 405 (2000), 767.

ferromagnet/antiferromagnet
Co/LaFeO₃ bilayer
interface exchange coupling
between the two materials

LaFeO₃ layer
XMLD Fe L₃

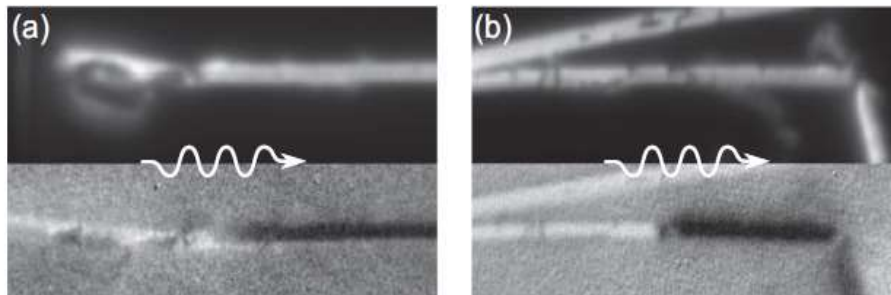
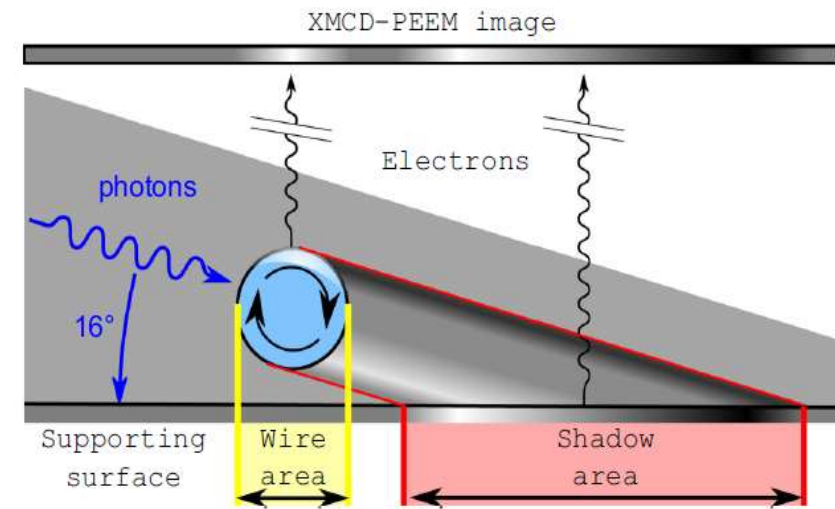


Co layer
XMCD Co L₃/L₂

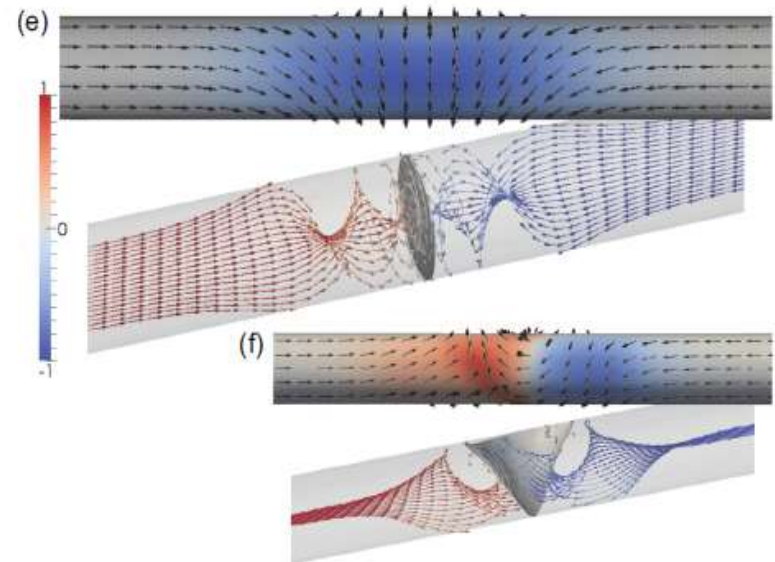
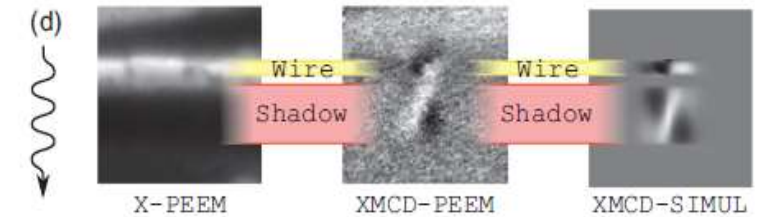
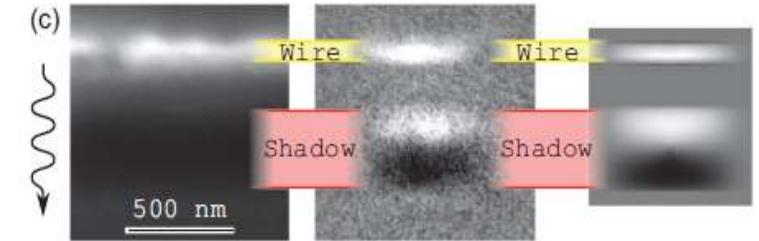


DW imaging in magnetic wires

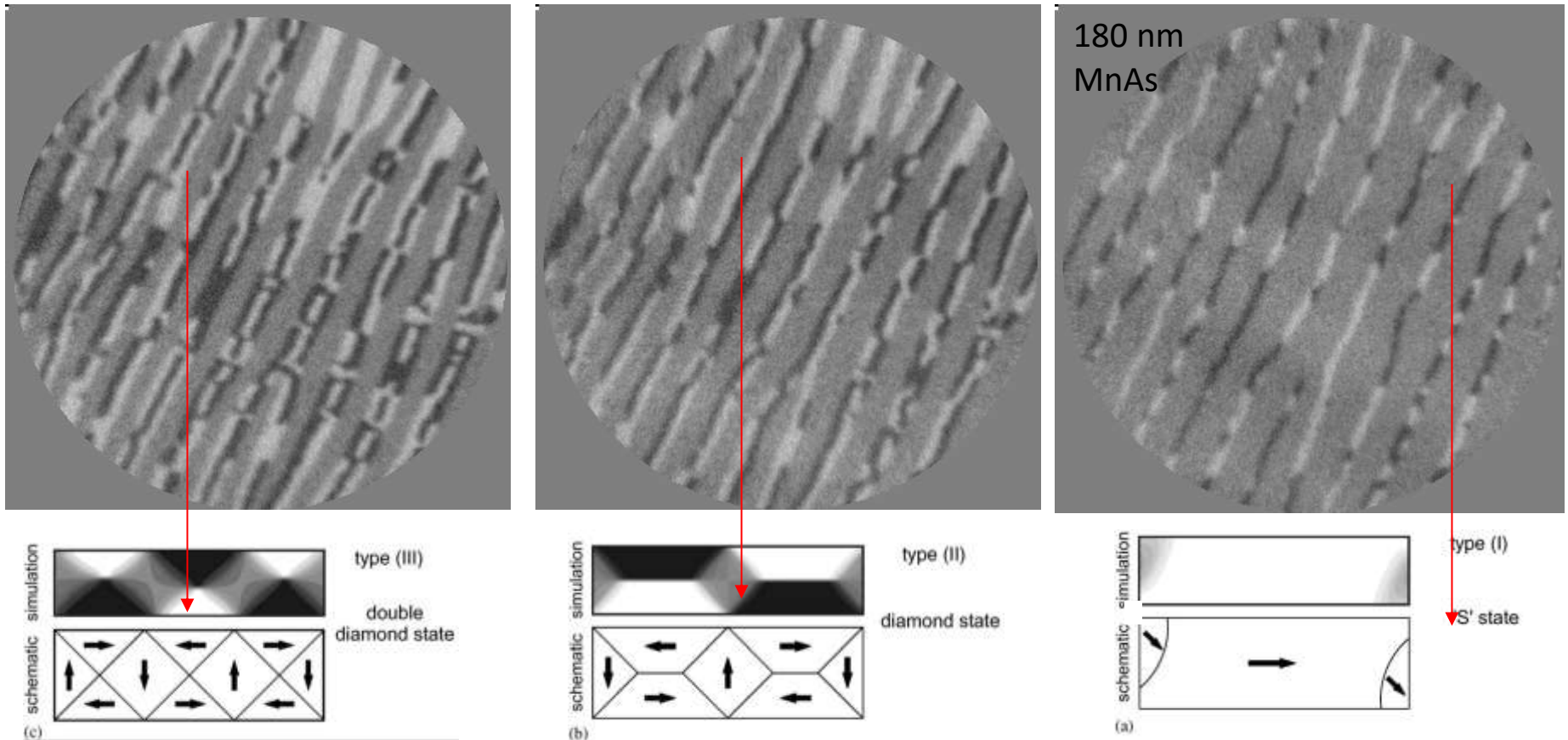
Observation of Bloch-point domain walls in cylindrical magnetic



wire



Experiment: Straight walls; Head to head domains



Simulation: Cross sectional cut: diamond state

R. Engel-Herbert et al, J. Magn. Magn. Mater. 305, (2006) 457



Adding the time domain to PEEM

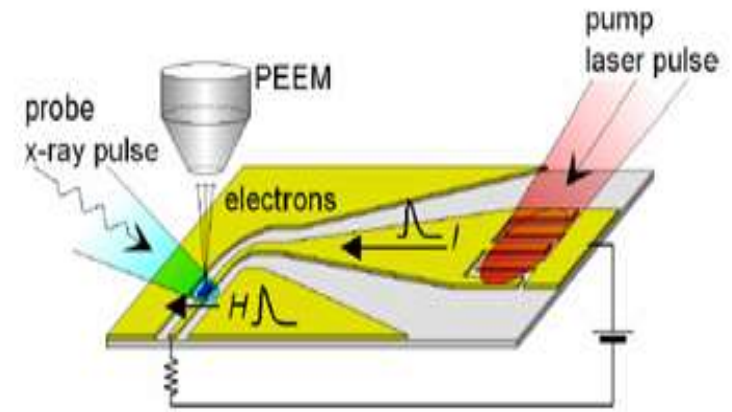
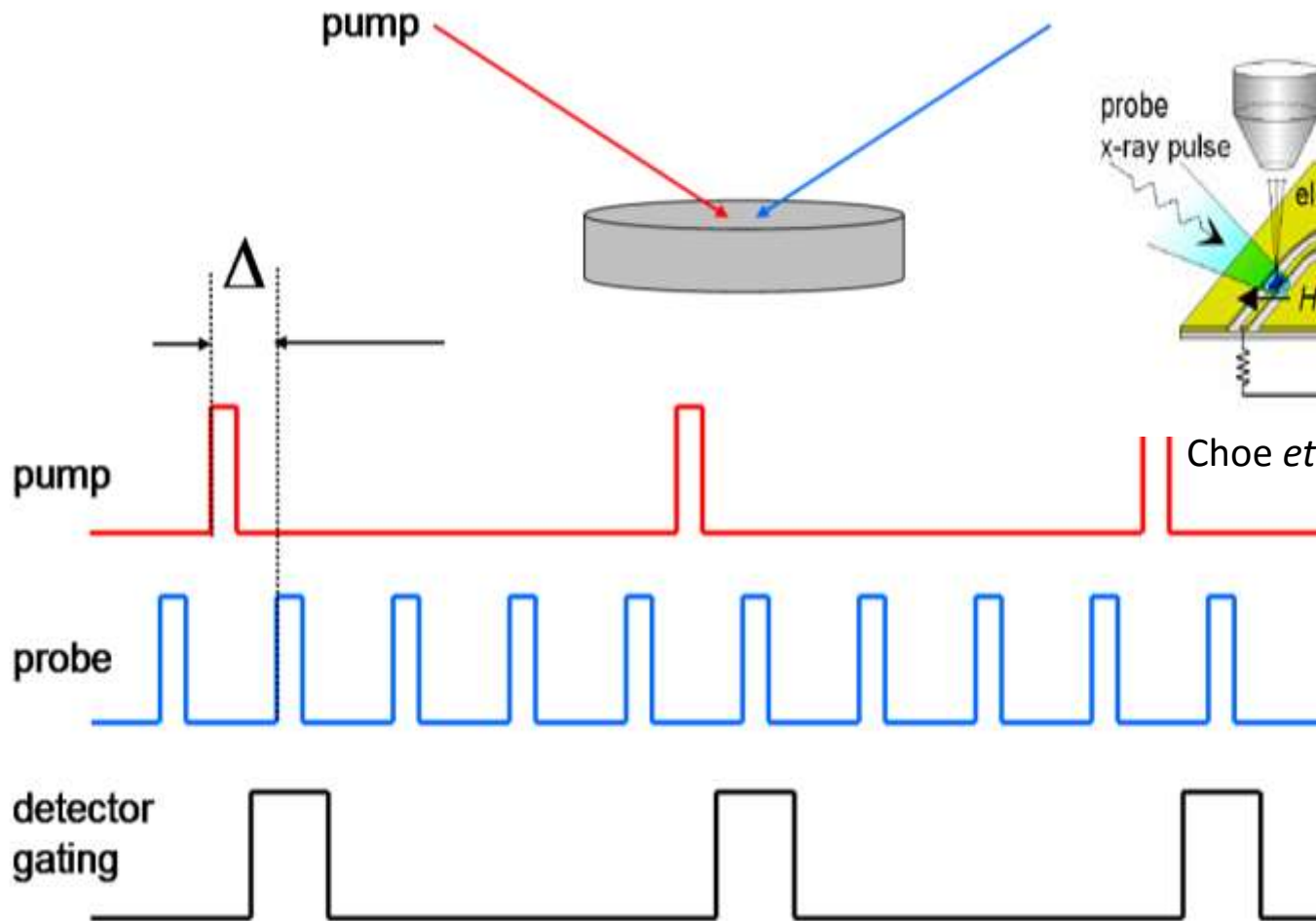
TR-PEEM methods

Time-resolved PEEM: the stroboscopic approach



Elettra Sincrotrone Trieste

Stroboscopic experiments combine high lateral resolution of PEEM with high time resolution, taking advantage of pulsed nature of synchrotron radiation

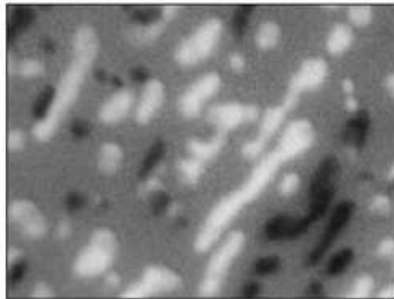


Choe *et al.*, Science 304, 420 (2004)

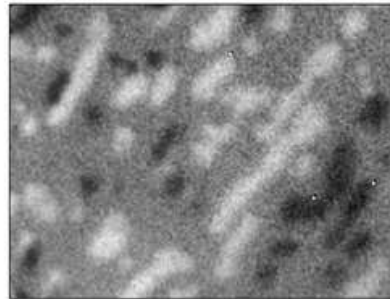
Detector gating for time-resolved XMCD PEEM



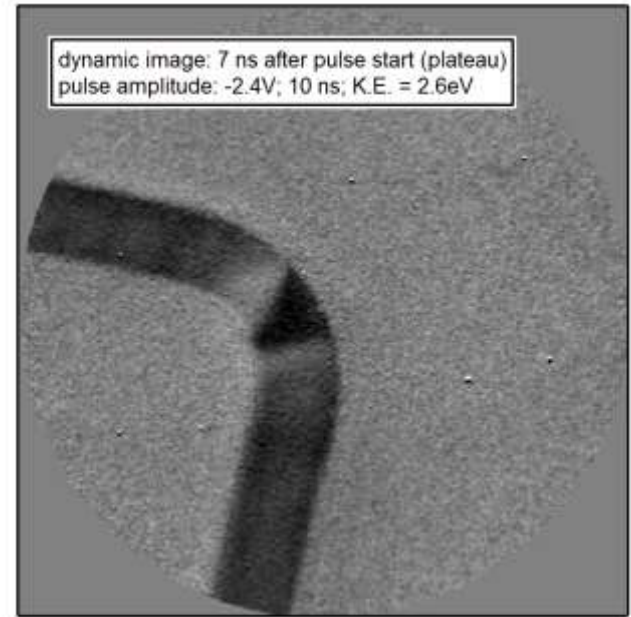
Elettra Sincrotrone Trieste



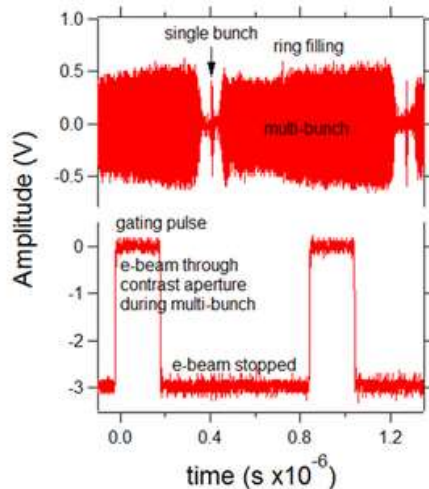
Multi-bunch image
32 images per helicity
Image exposure 4 s
Acquisition time: 5':18"



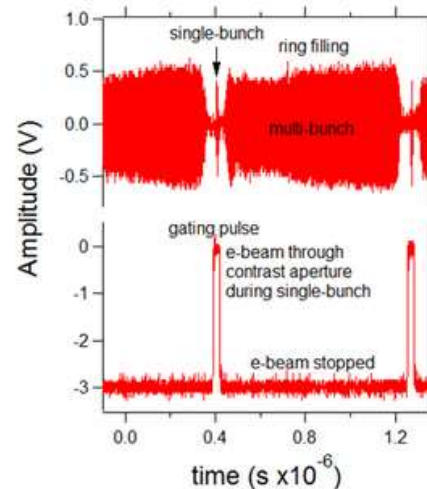
Single bunch image
24 images per helicity
Image exposure 20 s
Acquisition time: 17':40"



2 μm



pulse width 200 ns



pulse width 30 ns

Current-induced motion of magnetic domain walls in Permalloy (Fe₂₀Ni₈₀) nanostripes, through the spin-transfer torque (STT) effect. Our measurements reveal clear eformations of the domain wall shape

Quantitative Analysis of Magnetic Excitations in Landau Flux-Closure Structures Using Synchrotron-Radiation Microscopy

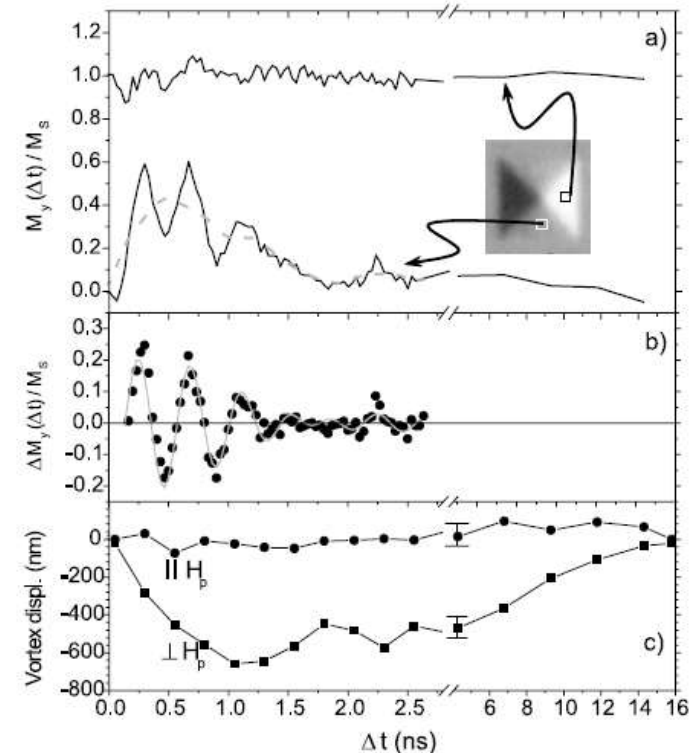
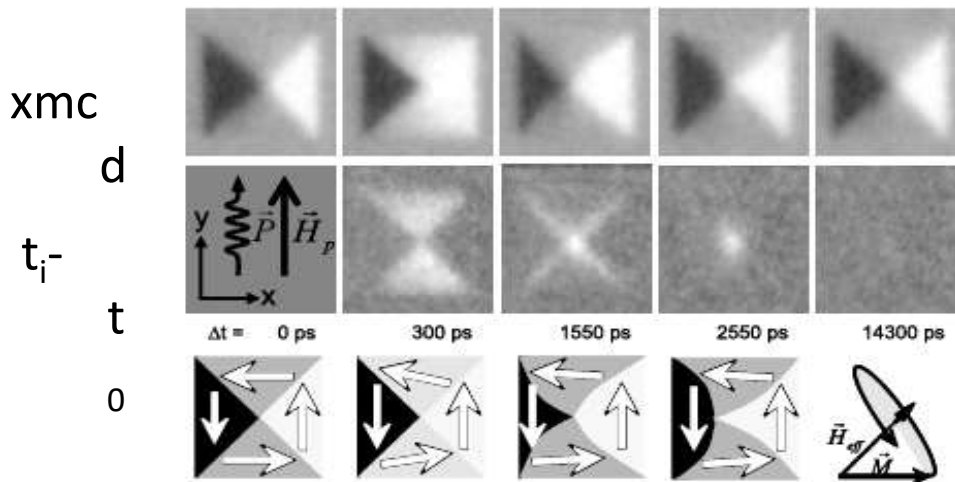
J. Raabe,^{1,*} C. Quitmann,¹ C. H. Back,² F. Nolting,¹ S. Johnson,¹ and C. Buehler¹

The time dependent magnetization is described by the phenomenological Landau-Lifshitz-Gilbert equation

$$\frac{d\vec{M}}{dt} = -\gamma_0 \vec{M} \times \vec{H}_{\text{eff}} + \frac{\alpha}{M} \left(\vec{M} \times \frac{d\vec{M}}{dt} \right).$$

The first term describes the precession of the magnetization \vec{M} about the total effective field \vec{H}_{eff} . The second term describes the relaxation back into the equilibrium state using the dimensionless damping parameter α .

torque $\vec{T} = -\gamma_0 \vec{M} \times \vec{H}_{\text{eff}}$



- XPEEM is a versatile full-field imaging technique. Combined with SR it allows us to implement laterally resolved versions of the most popular x-ray spectroscopies taking advantage of high flux of 3rd generation SR light sources.
- In particular, XAS-PEEM combines element sensitivity with chemical sensitivity (e.g. valence), and, more importantly, magnetic sensitivity. Magnetic imaging has been the most successful application of PEEM (next tutorial lecture!).
- XPEEM or energy-filtered PEEM adds true chemical sensitivity to PEEM. Modern instruments allow to combine chemistry with electronic structure using ARUPS.
- XPEEM can be complemented by LEEM, which adds structure sensitivity and capability to monitor dynamic processes.
- Lateral resolution will approach the nm range as AC instruments become available. Limitations due to space charge are not yet clear
- Novel application fields are being approached, such as biology, geology and earth sciences. HAXPES will increase our capabilities to probe buried structures (bulk).

Reviews and topical papers on x-ray spectromicroscopy and XPEEM

- S. Guenther, B. Kaulich, L. Gregoratti, M. Kiskinova, *Prog. Surf. Sci.* **70**, 187–260 (2002).
- E. Bauer, *Ultramicroscopy* **119**, 18–23 (2012).
- E. Bauer, *J. Electron. Spectrosc. Relat. Phenom.* (2012):
<http://dx.doi.org/10.1016/j.elspec.2012.08.001>
- G. Margaritondo, *J. Electron. Spectrosc. Relat. Phenom.* **178–179**, 273–291 (2010) .
- A. Locatelli, E. Bauer, *J. Phys.: Condens. Matter* **20**, 093002 (2008) .
- G. Schönhense *et al.*, in “*Adv. Imaging Electron Phys.*”, vol. **142**, Elsevier, Amsterdam, P. Hawkes (Ed.), 2006, pp. 159–323.
- G. Schönhense, *J. Electron. Spectrosc. Relat. Phenom.* **137–140**, 769 (2004) .
- C.M. Schneider, G. Schönhense, *Rep. Prog. Phys.* **65**, R1785–R1839 (2002) .
- W. Kuch, in “*Magnetism: A Synchrotron Radiation Approach*”, Springer, Berlin, E. Beaurepaire *et al.* (Eds.), 2006, pp. 275–320.
- J. Feng, A. Scholl, in P.W. Hawkes, “*Science of Microscopy*”, Springer, New York, J.C.H. Spence (Eds.), 2007, pp. 657–695.
- E. Bauer and Th. Schmidt, in “*High Resolution Imaging and Spectroscopy of Materials*”, Springer, Berlin, Heidelberg, F. Ernst and M. Rühle (Eds.), 2002, pp. 363–390.
- E. Bauer, *J. Electron Spectrosc. Relat. Phenom.* **114–116**, 976–987 (2002).
- E. Bauer, *J. Phys.: Condens. Matter* **13**, 11391–11405 (2001).